Cyclooxygenase 2 is a key enzyme for inflammatory cytokine-induced angiogenesis

TAKASHI KUWANO,* SHINTARO NAKAO,* HIDETAKA YAMAMOTO,† MASAZUMI TSUNEYOSHI,† TOMOYA YAMAMOTO,‡ MICHIHIKO KUWANO,§ AND MAYUMI ONO*,[1]

Departments of *Medical Biochemistry, †Anatomic Pathology, Pathological Sciences, and ‡Otorhinolaryngology, Graduate School of Medical Sciences, Kyushu University, Higashi-ku, Fukuoka 812-8582, Japan; and §Research Center for Innovative Cancer Therapy, Kurume University, Kurume, Fukuoka 830-0011, Japan

ABSTRACT **Cyclooxygenase1 (COX1) and COX2 mediate the rate-limiting step in arachidonic acid metabolism. Expression of COX2 mRNA and protein is often enhanced in various human cell types by inflammatory cytokines such as interleukin-1β (IL-1β) and tumor necrosis factor α (TNFα). IL-1β enhanced expression of various prostanoids and this expression was blocked by COX2 selective inhibitors. IL-1β markedly induced angiogenesis in vitro and in vivo, which was significantly inhibited by COX2 selective inhibitors but not by a vascular endothelial growth factor (VEGF) receptor tyrosine kinase inhibitor. In contrast, COX2 selective inhibitors only partially blocked VEGF-induced angiogenesis. EP2, EP4 (prostaglandin E2 receptors) agonists and thromboxane A2 (TXA2) receptor agonists induced angiogenesis in vitro and in vivo; IL-1β-induced angiogenesis was blocked by an EP4 antagonist and a TXA2 receptor antagonist. IL-1β induced much less angiogenesis in cornea of COX2 knockout mice than that of wild-type mice. This is the first report that COX2 and some prostanoids play a key role in IL-1β-induced angiogenesis.—Kuwano, T., Nakao, S., Yamamoto, H., Tsuneyoshi, M., Yamamoto, T., Kuwano, M., Ono, M. Cyclooxygenase 2 is a key enzyme for inflammatory cytokine-induced angiogenesis. *FASEB J.* 18, 300–310 (2004)**

Key Words: COX2 · vascular endothelial growth factor · prostanoid · inflammatory disease

BOTH ISOFORMS of cyclooxygenase (COX), constitutive COX1 and inducible COX2, catalyze the production of prostanoids from arachidonic acid (1). COX2-induced production of prostanoids is often implicated in inflammatory diseases, characterized by edema and tissue injury due to the release of many inflammatory cytokines and chemotactic factors, prostanoids, leukotrienes, and phospholipase (2, 3). Enhanced COX2-induced synthesis of prostaglandins stimulates cancer cell proliferation (4), promotes angiogenesis (5, 6), inhibits apoptosis (7), and increases metastatic potential (8). COX2 is also closely involved in the carcinogenesis process (9) and is overexpressed in adenocarcinoma in comparison with noncancerous mucosal regions in colon cancers (10) and gastric cancers (11). Elevated levels of mRNA and protein of COX2 are known to be associated with esophageal, head and neck, breast, lung, prostate, and other cancers, indicating a close involvement of COX2 in tumor progression and other pathological phenotypes in various malignant tumors (6, 9). COX2 is also known to be associated with lymph node metastasis in gastric cancer (12) and to affect the prognosis in primary lung adenocarcinoma (13).

On the other hand, ovulation is closely controlled by prostaglandins (14). Mice deficient in COX2 fail to ovulate, and this ovulatory failure could be restored by prostaglandin E2 (PGE2) or IL-1β and gonadotropins (15), suggesting that IL-1β/PGE2 plays a key role in ovulation. Numerous cytokines, hormones, growth factors, and chemical stimuli up-regulate expression of COX2 in various cell types including malignant cells, stromal cells, epithelial cells, and nonepithelial cells (9). Of these many stimuli, IL-1β has been well known to stimulate COX2 expression and/or PGE2 production in various cell types including monocytes/macrophages (16), vascular endothelial cells (17), colon fibroblasts (18), neuroblastoma cells (19), and osteoblasts (20). IL-1β-induced activation of the COX2 gene is modulated by various transcription factors such as NF-κB, IL-6, CRE (17, 21, 22). We have reported that potent angiogenic factors such as VEGF, IL-8, basic fibroblast growth factor (bFGF), metalloproteinases, and plasminogen activators are up-regulated in response to a representative inflammatory cytokine, TNFα in endothelial cells (23). In human cancer cells, IL-1α/β resulted in enhanced production of angiogenic factors VEGF and IL-8 (24). These findings led us to theorize that angiogenesis induced by TNFα and/or IL-1α/β is partially attributable to the production of such angiogenic factors (25). It remains unclear, how-

[1] Correspondence: Department of *Medical Biochemistry, Graduate School of Medical Sciences, Kyushu University, Maidashi 3-1-1, Higashi-ku, Fukuoka 812-8582, Japan. E-mail: mayumi@biochem1.med.kyushu-u.ac.jp

doi: 10.1096/fj.03-0473com

0892-6638/04/0018-0300 © FASEB

ever, whether representative inflammation-related substances such as prostanoids play any role in inflammatory angiogenesis.

A recent highlight is the development of COX2 inhibitors, known as nonsteroidal anti-inflammatory drugs (NSAIDs). Clinical trials of these NSAIDs have been performed for some inflammatory diseases such as rheumatoid arthritis and osteoarthritis (26, 27). NSAIDs have been shown to inhibit the growth of human colon tumor cells expressing higher levels of COX2 in vitro as well as in vivo (28). Treatment with NSAIDs decreased polyp number and size in familial adenomatous polyposis patients, indicating that NSAIDs may be chemopreventive against human polyposis (29). COX2 inhibitors markedly reduced polyposis in adenomatous polyposis coli (Apc) mice (30, 31), suggesting that selective COX2 inhibitors have potential as chemopreventive agents against human intestinal and colon cancer. One possible mechanism by which NSAIDs could modulate carcinogenesis, tumor growth, and other malignancy-related phenotypes in various tumors is their effects on tumor angiogenesis (9). Using animal models with Apc mutations during polyp formation, selective COX2 inhibitors decreased the expression of VEGF, a potent angiogenic factor (31). Overexpression of COX2 in colon cells is accompanied by up-regulation of VEGF, bFGF, nitric oxide synthases, and angiogenesis (6). COX2 inhibitors suppress both angiogenesis and tumor growth of xenografts of cancer cells in vivo (32). It was reported that a COX2 inhibitor suppressed angiogenesis induced by bFGF in rat corneas (33). Their studies suggest that NSAIDs may modulate tumor growth and carcinogenesis through antiangiogenesis. However, the underlying mechanism by which NSAIDs inhibit angiogenesis remains unclear. In our present study, we examine whether COX2 is directly associated with angiogenesis using various angiogenesis models and present a plausible model in which a COX2 inhibitor specifically induces antiangiogenic activity.

MATERIALS AND METHODS

Agents used

One COX2 inhibitor (DFU) was obtained from Banyu Pharmaceutical Co., Tokyo, and another (JTE-522) from Japan Tobacco Inc., Tokyo. The characteristics of these COX2 inhibitors were previously reported (34, 35). The chemical structures of DFU and JTE522 are shown in Fig. 1. ONO-AE1-259 (a PGE2 receptor EP2 agonist), ONO-AE1-329 (a PGE2 receptor EP4 agonist), ONO-AE3-208 (an EP4 antagonist), ONO-NT-126 (TXA2 receptor antagonists, used for in vitro), and ONO-8809 (orally active type of ONO-NT-126, used for in vivo) were obtained from ONO Pharmaceutical Co, Tokyo. U46619 (a TXA2 receptor agonist) was purchased from Cayman Chemical Co. (Ann Arbor, MI, USA). IL-1β and VEGF were purchased from R&D Inc. (Minneapolis, MN, USA).

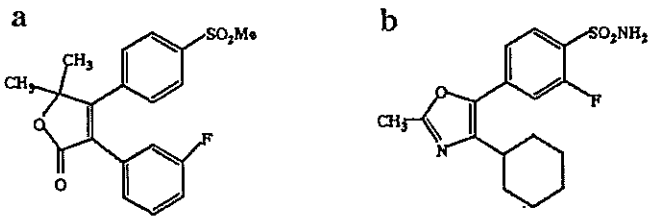

Figure 1. Chemical structures of COX2 inhibitors, DFU (*a*) and JTE522 (*b*). DFU and JTE522 are selective inhibitors of COX2 without significant activity on COX1. The chemical name of DFU ($C_{19}H_{17}FO_4S$; mol wt 360. 4) is 3-(3-fluorophenyl)-4(4-[methylsulfonyl] phenyl)-5, 5-dimethyl-5H-furan-2-one, and that of JTE522 ($C_{16}H_{19}FN_2O_3S$; mol wt 338. 4) is 4-(4-cyclohexyl-2-methyl-1, 3-oxazol-5-yl)-2-fluorobenzenesulfonamide.

Cell culture

HUVECs (Clonetics Inc., San Francisco, CA, USA) were cultured according to the manufacturer's instructions (36, 37).

Western blot analysis

Confluent KB3-1 cells were cultured in medium containing 2% NBS and HUVECs in medium containing 0.5% FBS for 24 h. The cells were then preincubated with COX2 inhibitors for 4 h before 1 ng/mL IL-1β or 20 ng/mL VEGF and incubated for 24 h at 37°C. Cells were then rinsed with ice-cold PBS and lysed in Triton X-100 buffer (50 μM HEPES, 150 μM NaCl, 1% Triton X-100, and 10% glycerol containing 1 μM PMSF, 1 mg/mL aprotinin, 1 mg/mL leupeptin, and 2 μM sodium vanadate). Cell lysates were subjected to SDS-PAGE and transferred to Immobilon membranes (Millipore, Bedford, MA, USA). After transfer, blots were incubated with the blocking solution and probed with anti-COX1 antibody, or anti-COX2 antibody, followed by washing. The protein content was visualized using HRP-conjugated secondary antibodies, followed by enhanced chemiluminescence (ECL, Amersham).

Migration assay of HUVECs

This assay was performed using a multiwell chamber. Polycarbonate filters (8 μm pores) were coated with 1.33 μg/mL fibronectin for 1 h at 37°C and used as the inner chamber (36, 37). HUVECs (3×10^5 cells) were suspended in EBM containing 0.5% FBS and seeded into the inner chamber. In the outer chamber, we added an EP4 agonist (ONO-AE1-329, 1 or 10 μM), a TXA2 receptor agonist (U46619, 1 or 10 μM), PGF2 (1 or 10 μM). VEGF (20 ng/mL), or IL-1β (1 ng/mL), with or without serial dilutions of DFU (10 or 100 μM) or JTE522 (10 or 100 μM). IL-1β, with or without EP4 antagonist (ONO-AE3-208, 1 or 10 μM) or TXA2 receptor antagonist (ONO-NT-126, 1 or 10 μM) in the same medium, was added. After incubation for 5 h at 37°C, nonmigrated cells on the upper surface of the filter were removed and cells that had migrated under the filter were counted. Cells were counted using average numbers from assays of three chambers.

Corneal micropocket assay in mice and quantification of corneal neovascularization

The corneal micropocket assay in mice has been described (36, 37). Briefly, 0.3 μL of hydron pellets (IFN Sciences, New

Brunswick, NJ, USA) containing IL-1β (30 ng/pellet), the EP2 agonist ONO-AE1-259 (1 or 10 μg/pellet), the EP4 agonist ONO-AE1-329 (1 or 10 μg/pellet), the TXA2 receptor agonist U46619 (50 or 100 μg/pellet), PGF2 (50 or 100 μg/pellet), or VEGF (200 ng/pellet) was prepared and implanted in the corneas of male BALB/c mice. DFU (50 $mg \cdot kg^{-1} \cdot day^{-1}$), JTE522 (50 or 100 $mg \cdot kg^{-1} \cdot day^{-1}$), the EP4 antagonist ONO-AE3-208 (1 $mg \cdot kg^{-1} \cdot day^{-1}$), and the TXA2 receptor antagonist ONO-8809 (1 $mg \cdot kg^{-1} \cdot day^{-1}$) were administered orally on days 1–6, and the VEGF receptor tyrosine kinase inhibitor SU5416 was administered intraperitoneally on days 1–6. On day 6, the mice were killed and their corneal vessels were photographed. Images of the corneas were recorded using Nikon Coolscan software. Areas of corneal neovascularization were analyzed using the software package NIH Image 1.61 (36, 37) and expressed in mm^2. The corneal micropocket assay was also performed with COX2 knockout mice. COX2 knockout mice (C57BL/6, 129P2-Ptgs2 ^{tm1smi}) (38) were purchased from Taconic Farms Inc. (Germantown, NY, USA). In this assay, 0.3 μL of hydron pellets containing IL-1β (30 ng/pellet) or VEGF (200 ng/pellet) were implanted in the corneas of male COX2 knockout or wild-type mice. As wild-type counterpart, C57 Black mouse was used.

ELISA assays of PGE2 and TXA2/TXB2

Concentrations of PGE2 and TXA2/TXB2 in the condition medium of HUVECs were measured using commercially available ELISA kits. Cells were plated in 24-well dishes in medium containing 2% FBS. When cells were subconfluent, the medium was replaced with 0.5% serum medium for 24 h. The cells were then preincubated with various concentrations of DFU or JTE522 for 4 h, followed by 1 ng/mL IL-1β at 37°C. Assays were performed after 24 h of incubation with 0.5% serum medium. Results were normalized for the number of cells and reported as picograms of growth factor/10^4 cells/24 h.

Immunohistochemistry of mouse cornea

After stimulation by IL-1β for 6 days, cornea of Balb/cN mouse was formalin-fixed, paraffin-embedded, and sliced into sections (4 μm thick) as described (39). Tissue sections were immunohistochemically stained using polyclonal primary antibody and the Streptavidin-biotin-peroxidase method (Histofine SABPO Kit; Nichirei, Tokyo, Japan). COX2 polyclonal antibody (Dilution 1:200; Cayman) was used as a primary antibody.

RESULTS

Enhanced expression of COX2 by IL-1β and effect of COX2 inhibitors

A representative inflammatory cytokine, IL-1β, induces up-regulation of COX2 in various cell types. Western blot analysis was performed with specific antibodies against COX1 and COX2 to examine expression of both isoforms in human head and neck cancer KB3-1 cells and HUVECs. In KB3-1 cells and HUVECs, IL-1β did not enhance COX1 protein expression, indicating a constitutive expression of COX1 gene (**Fig. 2*a***). Two COX2 inhibitors, DFU and JTE522, also had no effect on expression of COX1 protein. In contrast, there marked increases appeared in COX2 levels in KB3-1 cells as well as HUVECs by IL-1β. However, two COX2 inhibitors, DFU and JTE522, up to 50 μM did not block IL-1β-induced up-regulation of COX2 protein (Fig. 2*b*). Other inflammatory cytokines such as TNFα and IL-1α also enhanced production of COX2 protein but not that of COX1 (data not shown). IL-1β potently up-regulated expression of COX2 in various cell types used in this study. In contrast, VEGF, a representative angiogenic factor, did not enhance COX2 protein expression (Fig. 2*c*).

Production of prostanoids by IL-1β and effect of COX2 inhibitors

We first investigated whether IL-1β could enhance the production of prostanoids through the up-regulation of COX2 gene. HUVECs produce little if any prostanoids without the exogenous addition of cytokines (**Table 1**). IL-1β, however, induced marked production of prostanoids, including PGE2 and TXB2/TXA2. As TXA2 is very unstable, we therefore measured TXB2 (a relatively stable prostanoids derived from TXA2). Cellular production of both PGE2 and TXB2 was increased ~10-fold over the control by IL-1β alone. This IL-1β-induced production of these prostanoids was markedly inhibited by the addition of DFU or JTE-522 (Table 1). These two COX2 inhibitors were found to inhibit the production of prostanoids at similar dosages as used in this study when human cancer cells or monocytic cells were treated with IL-1β (data not shown).

Cell migration by vascular endothelial cells in response to IL-1β or prostanoids and effect of COX2 inhibitors

Cell migration of vascular endothelial cells is a key step in the process of neovascularization. We first examined whether IL-1β or prostanoids could stimulate cell migration and whether COX2 inhibitors could affect the IL-1β-induced migration of vascular endothelial cells. IL-1β at 1 ng/mL stimulated cell migration ~2.5-fold higher than the control, whereas VEGF at 20 ng/mL stimulated cell migration ~3.5-fold higher (**Fig. 3*a***). DFU or JTE522 at a concentration of 100 μM resulted in marked inhibition of IL-1β-induced migration by vascular endothelial cells (Fig. 3*a*). In contrast, there was no evidence of inhibition by DFU or JTE52 at 100 μM on cell migration stimulated by VEGF (Fig. 3*a*). Exogenous addition of a PGE2 receptor EP2 agonist (ONO-AE1-259), EP4 agonist (ONO-AE1-329), or a TXA2 receptor agonist (U46619) at a concentration of 10 μM stimulated cell migration ~twofold over the control (Fig. 3*b*). There was, however, no apparent stimulation of cell migration by PGF2 (data not shown). The stimulatory effects of prostanoids were comparable to those of VEGF or IL-1β, and their stimulatory effects on cell migration were reproducibly observed. We then investigated which prostanoid was responsible for IL-1β-induced angiogenesis in vitro. IL-1β-induced cell

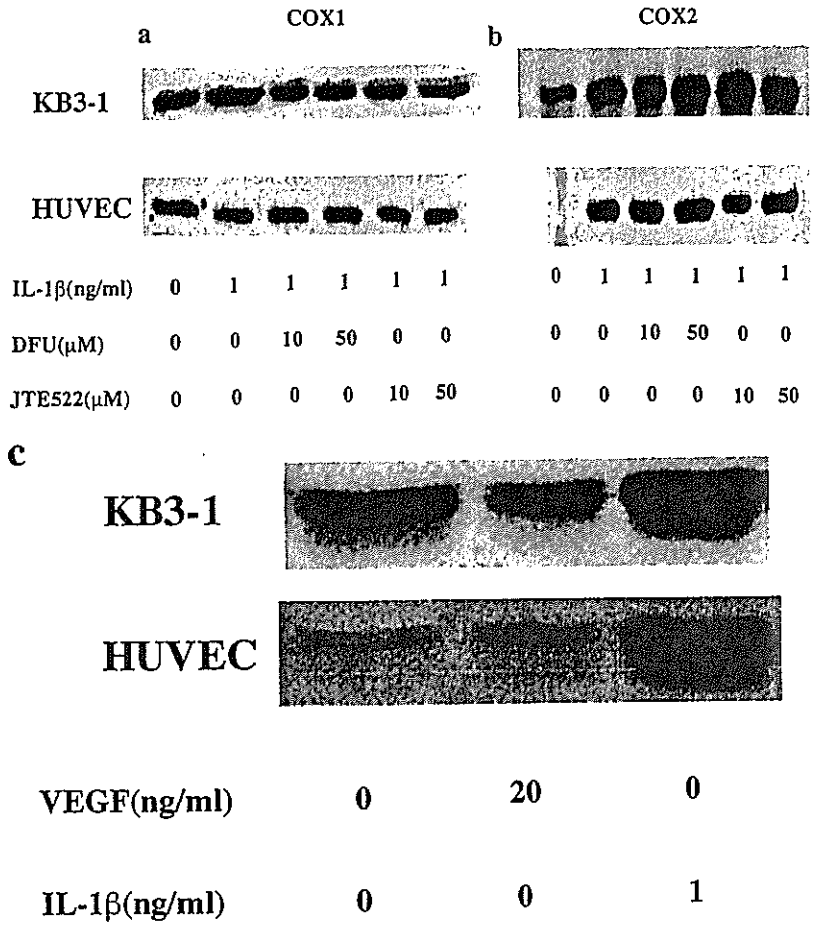

Figure 2. Effect of COX2 inhibitors on expression of COX1 and COX2 protein. Effects of COX2 inhibitors on protein expression of COX1 and COX2 protein in KB3-1 and HUVECs were compared by Western blot analysis. KB3-1 cells and HUVECs were incubated in the absence or presence of 1 ng/mL IL-1β with or without indicated doses of DFU or JTE522. The same amount of cellular protein was separated by SDS-PAGE and Western blot analysis was performed with specific antibody against COX1 (*a*) and COX2 (*b*). *c)* Protein levels of COX2 in KB3-1 cells and HUVECs were also compared when exposed to 20 ng/mL VEGF or 1 ng/mL IL-1β.

migration was significantly inhibited by an EP4 antagonist (ONO-AE3-208, 10 μM) and a TXA2 receptor antagonist (ONO-NT-126, 10 μM) (Fig. 3*c*). These findings suggest that COX2 activity is closely associated with IL-1β-induced angiogenesis in vitro. Moreover, TXA2 and PGE2 appeared to play critical roles in IL-1β-induced angiogenic activity in vitro.

TABLE 1. *IL-1β-induced production of prostanoids by vascular endothelial cells and inhibition of COX2 inhibitors*[a]

IL-1β (ng/mL)	COX2 inhibitor (μM)	PGE2 (pg/mL · 10^4 cells)	TXB2/TXA2 (pg/mL · 10^4 cells)
0	None	1.4	1.2
1	None	15.2 (100)[b]	15.8 (100)
1	DFU (0.3)	6.1 (34)	10.1 (61)
1	DFU (3.0)	4.8 (25)	5.9 (32)
1	DFU (30)	2.1 (5)	1.8 (4)
1	JTE522 (0.1)	6.9 (40)	10.5 (64)
1	JTE522 (1.0)	2.8 (10)	6.5 (35)
1	JTE522 (50)	2.4 (4)	2.0 (6)

[a] PGE2 and TXB2/TXA2 production into culture medium was measured by ELISA when HUVECs were stimulated with IL-1β and incubated with or without DFU or JTE522 for 24 h. [b] Each value (pg/mL · 10^4 cells/24 h) was the mean of duplicate cultures. In parentheses, IL-1β-induced production of prostanoids was recorded as 100% when cellular amounts of eicosanoids in the absence of the cytokine was subtracted from that in the presence of the cytokine alone.

Angiogenesis in vivo in response to IL-1β and the effect of selective COX2 inhibitors

We investigated whether IL-1β could induce angiogenesis in vivo in mouse corneas. Implantation of IL-1β at doses of 10–30 ng into mouse corneas was found to induce neovascularization in a nonvascular area of the cornea at rates comparable to 200 ng of VEGF. Apparent angiogenesis in the cornea in mice when either IL-1β at 30 ng or VEGF at 200 ng was implanted (Fig. 4*b, f*). Oral administration of DFU (50 mg · kg^{-1} · day^{-1}) or JTE522 (100 mg · kg^{-1} · day^{-1}) dramatically inhibited IL-1β-induced angiogenesis (Fig. 4*c, d*) but not VEGF-induced angiogenesis (Fig. 4*h*). In contrast, intraperitoneal administration of SU5416, a specific inhibitor of both VEGF receptors, KDR/Flk-1 and Flt-1 (40), almost completely inhibited VEGF-induced angiogenesis (Fig. 4*g*) but had no effect on IL-1β-induced angiogenesis in vivo (Fig. 4*e*). Quantitative analysis using three or four mice for each assay showed almost complete inhibition of IL-1β-induced neovascularization when DFU or JTE-522 was orally administered (Fig. 4*i*). Almost no inhibition by DFU (Fig. 4*h, i*) or JTE-522 (data not shown) of VEGF-induced neovascularization was observed, whereas SU5416 significantly inhibited VEGF-induced neovascularization. IL-1β-induced angiogenesis was blocked by selective COX2 inhibitors in vitro and in vivo.

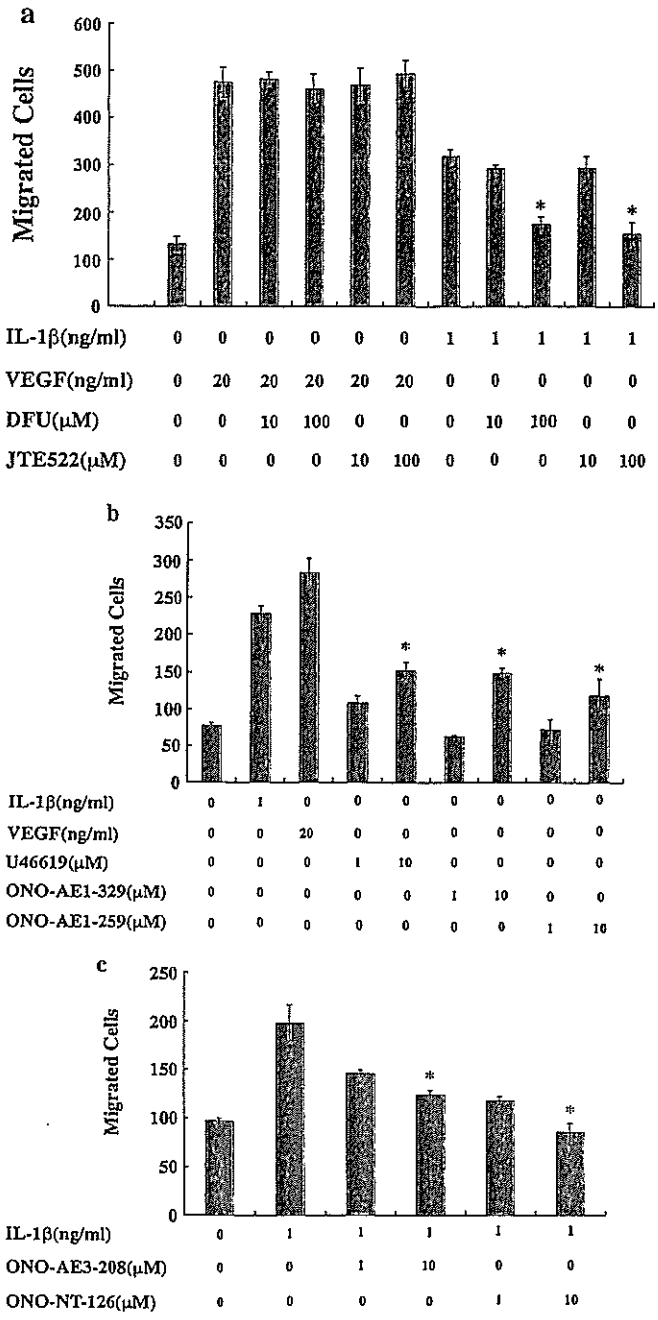

Figure 3. Effects of COX2 inhibitors and prostanoids on cell migration. *a)* Effects of COX2 inhibitors on endothelial cell migration by VEGF and IL-1β were assayed using HUVECs in vitro. The migrated cell number was the mean of triplicate dishes. Relative activity (%) was recorded as 100% when the cell number (133±9.7) in the absence of any factor was subtracted from that in the presence of VEGF (20 ng/mL) or IL-1β (1 ng/mL) alone. *b)* Effects of a TXA2 receptor agonist (U46619, 1 or 10 μM), a PGE2 receptor EP2 agonist (ONO-AE1-259, 1 or 10 μM) and EP4 agonist (ONO-AE1-329, 1 or 10 μM) on cell migration were determined by using HUVECs. *c)* Effects of a TXA2 receptor antagonist (ONO-NT-126) and an EP4 antagonist (ONO-AE3-208) on IL-1β-induced vascular endothelial cell migration. Both agents were found to significantly inhibit IL-1β-induced cell migration in vitro. Each column gives the average value ±SD when 3 independent assays were performed. *Statistically significant difference ($P<0.01$) to value for IL-1β alone.

Angiogenesis in vivo by prostanoid receptor agonists

We next investigated whether prostanoids could also induce neovascularization in mouse corneas in vivo. Corneal implantation of a TXA2 receptor agonist (U46619, 50 or 100 μg), an EP2 receptor agonist (ONO-AE1-259, 1 or 10 μg) or an EP4 receptor agonist (ONO-AE1-329, 1 or 10 μg) as a pellet was found to induce angiogenesis, although its neovascularization activity was less than that of IL-1β (Fig. 5*c–e*). In contrast, PGF2 did not induce angiogenesis (data not shown). Quantitative analysis using three or four mice for each assay showed angiogenic activity of TXA2 and PGE2 when their respective agonists were implanted (Fig. 5*f*).

Effect of prostanoid receptor antagonists on angiogenesis in vivo by IL-1β

We further investigated which prostanoid was most closely involved in IL-1β-induced angiogenesis. Oral administration of the TXA2 receptor antagonist ONO-8809 (1 mg · kg^{-1} · day^{-1}) or the EP4 receptor antagonist ONO-AE3-208 (1 mg · kg^{-1} · day^{-1}) was found to reduce IL-1β-induced angiogenesis in mouse corneas (Fig. 6*a–c*). Quantitative analysis showed that ONO-8809 and ONO-AE3-208 both significantly inhibited IL-1β-induced angiogenesis by ~50% (Fig. 6*d*).

Localization of COX2 in infiltrating cells within IL-1β–treated corneas

We examined whether COX2-positive cells were infiltrated in IL-1β-treated corneas. The cornea developed new vessels by IL-1β, immunohistochemical analysis of the corneas was performed with anti-COX2 antibody. Many infiltrating cells stained with COX2 appeared in the stroma and anterior chamber when treated with IL-1β (Fig. 7). By contrast, there appeared to be no infiltrating cells within the untreated corneas (data not shown). Cells infiltrated near new vessels in the cornea consisted of inflammatory cells, including monocyte/macrophage. Immunohistochemical analysis with murine macrophage-recognizing monoclonal antibody (F4/80) showed many F4/80-positive cells in IL-1β-treated cornea (data not shown).

Angiogenesis by IL-1β in COX2 knockout mice

We finally asked whether COX2 was directly involved in IL-1β-induced angiogenesis in vivo. We compared angiogenesis by IL-1β between COX2 knockout mice and wild-type mice. Implantation of IL-1β at a dose of 30 ng into cornea of wild-type mouse induced neovascularization in a nonvascular area. By contrast, a marked reduction in the angiogenesis in cornea of COX2 knockout mice was demonstrated (Fig. 8*b*). We observed angiogenesis at similar levels between wild-type and COX2 knockout mice by VEGF at a dose of 200 ng (Fig. 8*c, d*). Quantitative analysis using three to four

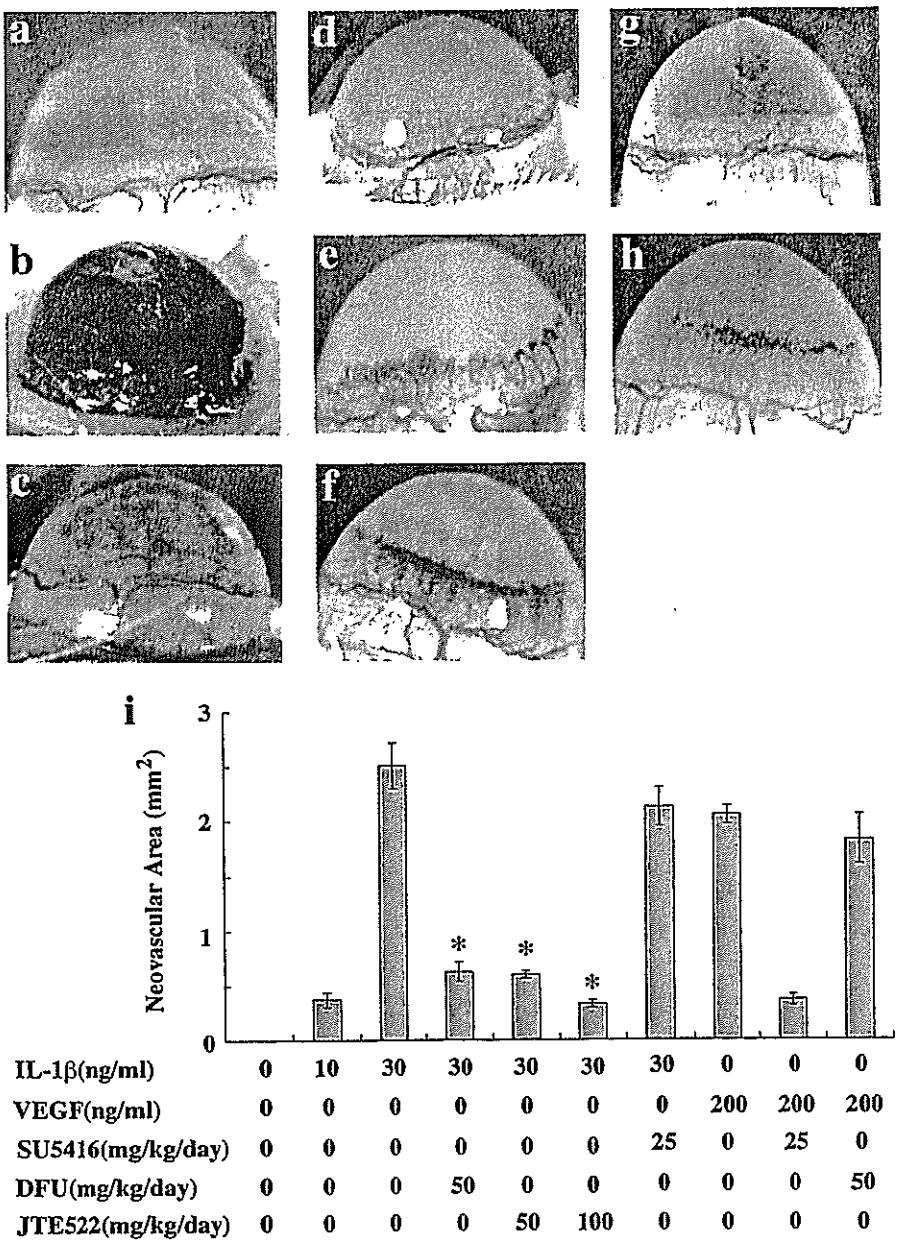

Figure 4. Effects of COX2 inhibitors on angiogenesis in vivo. Photographs of angiogenesis in mouse corneas. Mice were treated with DFU (50 mg · kg^{-1} · day^{-1}, orally), JTE522 (50 or 100 mg · kg^{-1} · day^{-1}, orally), or SU5416 (25 mg · kg^{-1} · day^{-1}, intraperitoneally) on day 1 to 6. Six days later, vessels in the region of the pellet implant were photographed. Representative photographs of mouse corneas; *a)* buffer alone, *b)* IL-1β (30 ng), *c)* IL-1β with DFU (50 mg · kg^{-1} · day^{-1}), *d)* IL-1β with JTE522 (100 mg · kg^{-1} · day^{-1}), *e)* IL-1β with SU5416 (25 mg · kg^{-1} · day^{-1}), *f)* VEGF (200 ng), *g)* VEGF with SU5416 (25 mg · kg^{-1} · day^{-1}), *h)* VEGF with DFU (50 mg · kg^{-1} · day^{-1}). *i)* Quantification of corneal neovascularization in mice after administration of DFU, JTE522, or SU5416. Neovascular areas developed in mouse corneas (*a–h*) were quantified as described in Materials and Methods. Columns are mean (±SD) of 3 or 4 independent experiments. *Statistically significant difference ($P<0.01$) to value for IL-1β alone.

mice for each assay showed very low (~20%) angiogenesis by IL-1β in COX2 knockout mice in comparison with wild-type mice (Fig. 8*e*). A similar level of angiogenic activity in vivo by VEGF between COX2 knockout and wild-type mice was observed (Fig. 8*e*).

DISCUSSION

Voronov et al. recently reported that IL-1 is required for both angiogenesis and tumor invasiveness using IL-1β or IL-1α knockout mice (41). Other independent studies have reported that IL-1β promotes tumor growth, invasion, and angiogenesis in animal models with concomitant enhanced production of VEGF, MMP-2, IL-8, and adhesion molecules (42, 43). IL-1α also promotes angiogenesis in vivo through VEGF receptor pathway possibly by inducing VEGF synthesis (44). However, it remains unclear how VEGF or other angiogenesis-related factors could be involved in IL-1-induced angiogenesis and tumor invasion. In our present study, IL-1β was found to markedly enhance production of prostanoids such as PGE2 and TXA2/TXB2. IL-1β-induced production of prostanoids was almost completely blocked by both COX2-selective inhibitors DFU and JTE522. Both cell migration by vascular endothelial cells in vitro and corneal neovascularization in vivo were markedly induced in response to IL-1β at rates similar to VEGF. Administration of COX2 inhibitors resulted in a dramatic reduction of IL-1β-induced angiogenesis in vivo as well as cell migration in vitro. A TXA2 receptor agonist (U46619), an EP2 agonist (ONO-AE1-259), and an EP4 agonist (ONO-AE1-329) stimulated cell migration in vitro and induce corneal neovascularization in mice. TXA2 receptor antagonists (ONO-8809) and EP4 antagonist

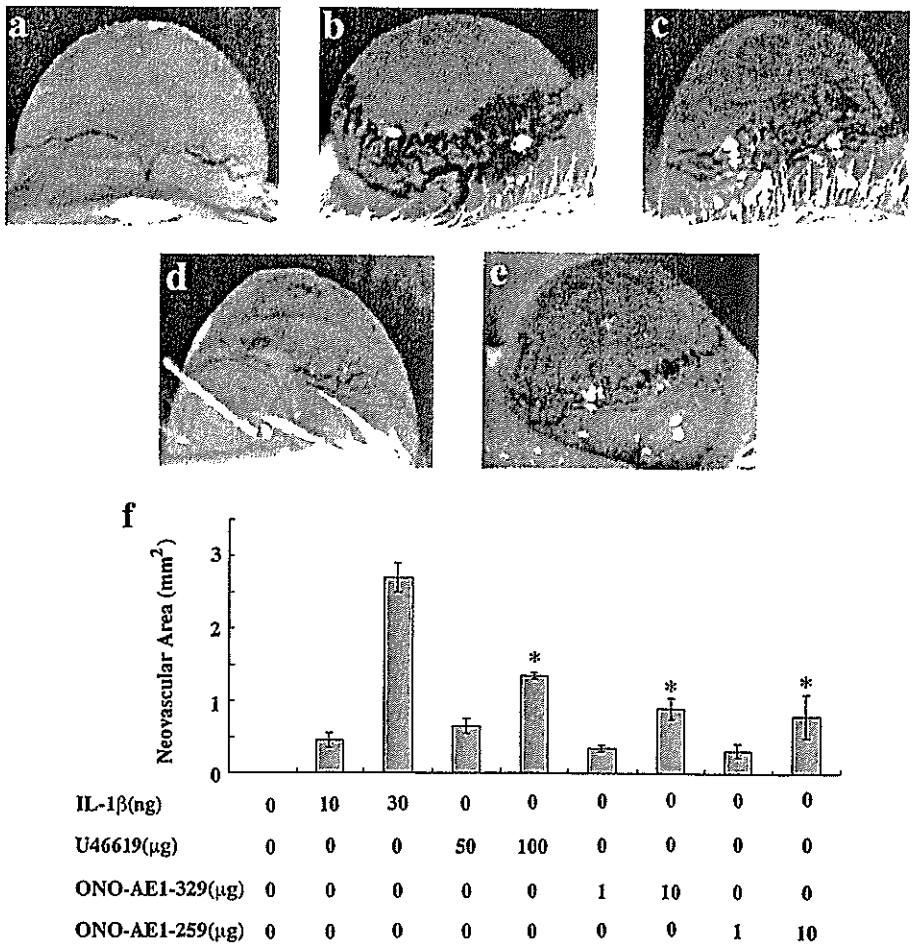

Figure 5. Angiogenesis in vivo by prostanoid receptor agonists. Photographs of angiogenesis in mouse corneas. Hydron pellets containing of *a)* buffer alone, *b)* IL-1β (30 ng/pellet), *c)* TXA2 receptor agonist (U46619, 100 μg/pellet), *d)* EP2 agonist (ONO-AE1-259, 10 μg/pellet), *e)* EP4 agonist (ONO-AE1-329, 10 μg/pellet) were implanted into the corneas of Balb/c mice. Six days later vessels in the region of the pellet implanted were photographed. Quantitative analysis was performed on data in panel *f* with 3 or 4 mice corneas.

(ONO-AE3-208) also inhibited IL-1β-induced angiogenesis in vivo. We therefore present a model that some prostanoids such as TXA2 and PGE2 directly induce angiogenesis through interaction with their cognate receptors on vascular endothelial cells (**Fig. 9**).

We also observed apparent reduction in IL-1β-induced angiogenesis in corneas of the COX2 knockout mice in comparison with wild-type mice. This experiment with knockout mice strongly suggests a direct involvement of COX2 and relevant prostanoids in

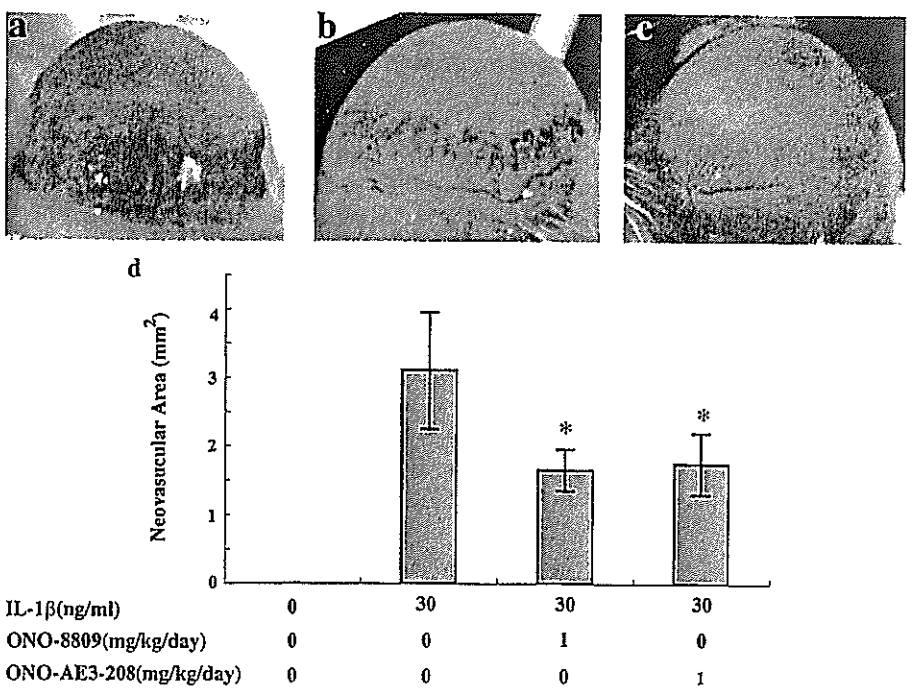

Figure 6. Inhibition of IL-1β–induced angiogenesis by prostanoid receptor antagonists. Photographs of angiogenesis in mouse corneas. Hydron pellets containing IL-1β (30 ng/pellet) were implanted into the corneas of Balb/c mice. TXA2 receptor antagonist (ONO-8809, 1 mg · kg^{-1} · day^{-1}) or the PGE2 receptor EP4 antagonist (ONO-AE3-208, 1 mg · kg^{-1} · day^{-1}) was administered orally on day 1 to 6. Representative photographs of mouse corneas *a)* IL-1β (30 ng/pellet), *b)* IL-1β with ONO-8809 (1 mg · kg^{-1} · day^{-1}), and *c)* IL-1β with ONO-AE3-208 (1 mg · kg^{-1} · day^{-1}). *d)* Quantitative analysis was performed on data in panels *a–c* with 3 or 4 mice corneas. *Statistically significant difference ($P<0.01$) to value for IL-1β alone.

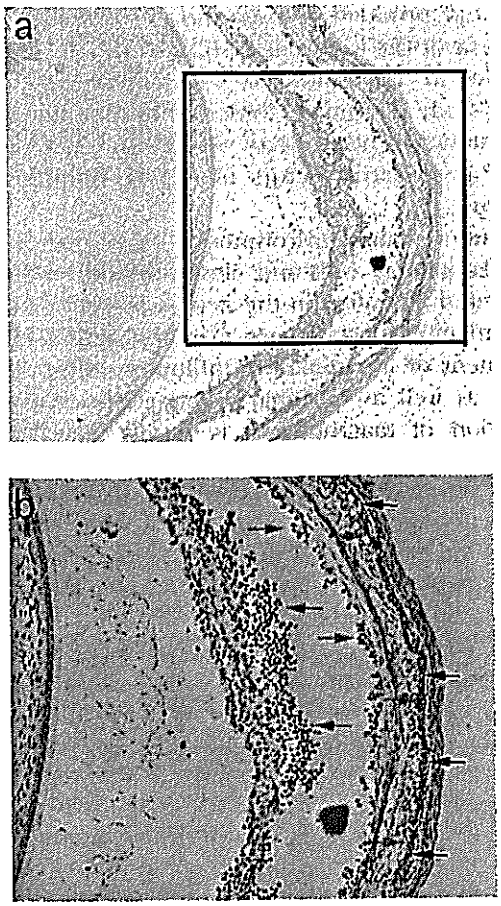

Figure 7. Identification of COX2-positive cells infiltrating in corneas treated with IL-1β. Immunohistochemical staining was preformed with the sections of IL-1β-treated cornea in mice with anti-COX2 antibody (*a, b*). The black arrows represent new vessels and the red arrows represent COX2 positive cells. Compared with untreated group (data not shown), section of IL-1β-treated corneas shows numerous immunopositive cells in stroma and anterior chamber. Magnification, 40× (*a*), 100× (*b*).

IL-1β-induced angiogenesis. However, some neovascularized area was observed in the COX2 knockout mice by IL-1β, suggesting an involvement of different factors or pathways in IL-1β-induced angiogenesis.

COX2 overexpresssion up-regulates expression of several angiogenic factors, VEGF and bFGF, and COX2 inhibitors significantly inhibited production of VEGF and bFGF as well as angiogenesis in vivo (32, 45). Administration of COX2 inhibitors blocked expression of VEGF and bFGF in vitro as well as angiogenesis and tumor growth in vivo (32). It has been reported that prostaglandins stimulate production of VEGF and bFGF (46). We have reported that IL-1α and TNFα significantly enhance production of VEGF, IL-8, bFGF (23, 24), and COX2 protein in endothelial cells and cancer cells (Fig. 9). Such potent angiogenic factors are expected to be involved in angiogenesis through the IL-1α/β-COX2 pathway (17). It seems likely there are at least two pathways in the IL-1β-induced production of VEGF and other factors through either COX2-dependent or COX2-independent pathways. IL-1β-induced production of VEGF and IL-8 was, however, inhibited by only ~50% when treated with COX2 inhibitors at concentrations of 50 to 100 μM (T. Kuwano and M. Ono, unpublished data). In contrast, COX2 inhibitors at low concentrations markedly inhibited IL-1β-induced production of PGE2 and TXB2/TXA2 (Table 1). Our in vivo study further demonstrated that IL-1β-induced corneal angiogenesis in vivo was blocked, but not completely, by DFU and JTE522. This IL-1β-induced angiogenesis was blocked only slightly if at all by SU5416. This in vivo study suggests specific involvement of prostanoids in IL-1β-induced angiogenesis rather than in angiogenesis by the VEGF/VEGF receptor pathway (Fig. 9).

Arachidonic acid metabolites have been known to modulate endothelial cell proliferation or migration

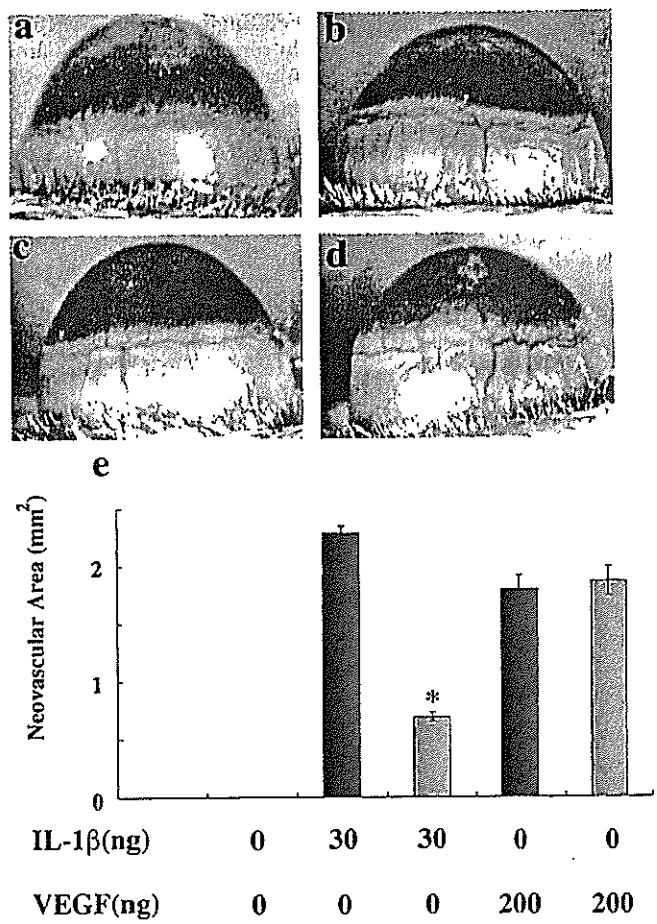

Figure 8. Angiogenesis in cornea of COX2 knockout mice Photographs of angiogenesis in mouse corneas. IL-1β or VEGF was implanted in corneas of COX2 knockout mice and wild-type mice on day 1. Six days later, vessels in the region of the pellet implanted were photographed. Representative photographs of angiogenesis in corneas of wild-type and COX2 knockout mice *a)* wild-type mouse: IL-1β (30 ng); *b)* COX2 knockout mouse: IL-1β (30 ng); wild-type mouse: VEGF (200 ng); and *d)* COX2 knockout mouse: VEGF (200 ng). *e)* Quantitative analysis was performed on data in panels *a–d* with 3 or 4 mice corneas. Black bars represent wild-type mice; blue bars represent COX2 knockout mice. *Statistically significant difference ($P<0.01$) to the value for IL-1β in wild-type mouse.

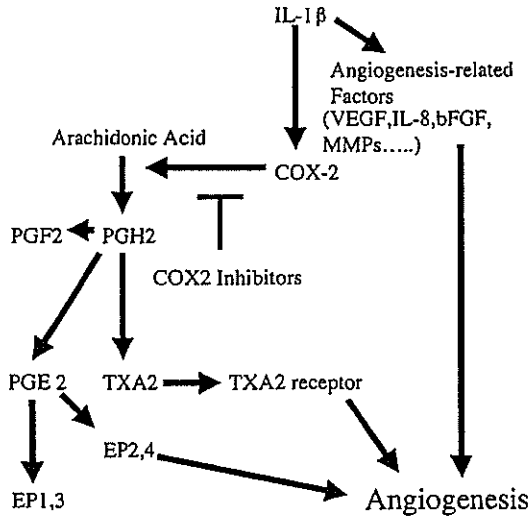

Figure 9. A model for IL-1β-induced angiogenesis and effect of COX2 inhibitor. We previously reported that IL-1β and TNF-α enhance production of angiogenesis-related factors such as VEGF, IL-8, bFGF, plasminogen activator, and metalloproteinases from vascular endothelial cells and other cell types, resulting in angiogenesis through autocrine and/or paracrine control. In the present study, we demonstrated that inflammatory cytokines such as IL-1β and probably TNF-α induce angiogenesis through the direct interaction of prostanoids with vascular endothelial cells. COX2 induced by IL-1β catalyzes the process of arachidonic acid cascade in vascular endothelial cells. PGE2 and TXA2 are prostanoids, final products of the arachidonic acid cascade thought to be critical factors for angiogenesis through PGE2 receptors (EP2, EP4) and the TXA2 receptor.

and capillary formation in vivo (47). We previously reported that arachidonic acid metabolism inhibitors block angiogenesis in vivo as well as in vitro, suggesting a close association between prostanoids and angiogenesis. Of the various prostanoids produced by COX2 in response to IL-1β, PGE2 appears to play a key role in inflammatory angiogenesis (5). PGI2 (48) and TXA2 (49) were reported to demonstrate some angiogenic activity in vivo. Our study indicated that PGE2 and TXA2 stimulate cell migration by vascular endothelial cells. Cell migration in response to IL-1β, but not to VEGF, was blocked by DFU or JTE522. Angiogenesis assay in vivo also demonstrated induction of angiogenesis in corneas by a TXA2 receptor agonist (U46619) and an EP4 agonist (ONO-AE-329). Taken together, these results consistently support the notion that inflammatory cytokine-elicited angiogenesis is induced mainly by TXA2, PGE2, and other undetermined prostanoids through COX2 activation. Both COX2 inhibitors at low concentrations significantly inhibited the production of PGE2 and TXA2/TXB2 whereas at high concentrations inhibited the IL-1β-induced migration of vascular endothelial cells (Table1 and Fig. 3). Concerning this discrepancy, experimental conditions for the two assay systems are different. *1)* In the migration assay, IL-1β and COX2 inhibitors were added simultaneously while COX2 inhibitors were added 4 h before exposure to IL-1β in the prostanoid production assay. *2)* Migration assay was performed for only 5 h whereas prostanoid production assay was performed for 24 h. We still favor the idea that PGE2 and TXA2/TXB2 play key roles in IL-1β-induced cell migration. However, further study is required to determine the involvement of prostanoids other than PGE2 and TXA2/TXB2 and/or angiogenic factors in the IL-1β-induced cell migration.

The tumor microenvironment consists mainly of various inflammatory cells and closely affects proliferation, survival and migration in the neoplastic process (50). Of these inflammatory cell types, macrophage is a significant component of inflammatory infiltrates, affecting angiogenesis as well as malignant characteristics of cancer. Infiltration of macrophages is closely associated with microvascular density and malignant status in various human tumor types (24). Activated macrophages are thought to play a key role in angiogenesis of inflammatory diseases and in malignant tumors. Activated macrophages infiltrating tumor stroma and inflammatory regions produce various angiogenesis factors, including prostanoids (25). Related studies have reported that activation of macrophage is accompanied by induction of COX2 and IL-1β (16) and that high expression of COX2 is often observed in macrophages infiltrating in tumor stroma (18). We have reported that macrophage infiltration is maximized in mouse cornea within 4 to 5 days after inflammatory stimuli by chemical cauterization and that the kinetics of macrophage infiltration is similar to that of neovascularization (39). Consistent with this study, inflammatory cytokine IL-1β could induce infiltration of COX2-positive macrophages and/or other inflammatory cells in cornea. If such macrophages/monocytes actively produce prostanoids, these prostanoids could also play a key role in angiogenesis under certain inflammatory conditions.

NSAIDs block tumor development in some animal carcinogenesis models (30). In a recent study, COX2 overexpression in the skin of transgenic mice resulted in suppression of tumor development, again suggesting a key role for COX2 and elevated prostaglandin levels in the development of skin tumor (51). On the other hand, angiogenesis, a risk factor for metastasis and recurrence (52), is closely involved in the tumor development process. Angiogenesis is a prerequisite for the early switch-on of tumor development in several animal carcinogenesis models. Anticarcinogenic and antineoplastic effects of NSAIDs are known to be mediated through COX2-dependent and -independent pathways (53). Anticarcinogenesis and antineoplastic effects through inhibition of COX2 dependent pathways could be attributable at least in part to inhibition of angiogenesis by NSAIDs. The clinical application of COX2 inhibitors will provide new information as to whether COX2 is a useful molecular target. FJ

We would like to thank Banyu Pharmaceutical Co. and Japan Tobacco Inc. for COX2 inhibitors and ONO Pharmaceutical Co. for prostanoid receptor agonists and antagonists. This work was supported by grants for cancer research from the Ministry of Education, Science, Sport and Culture, Japan (M.O., M.K.), and the Ministry of Human Health Labor and Welfare, Japan (M.K.).

REFERENCES

1. Williams, C. S., and DuBois, R. N. (1996) Prostaglandin endoperoxide synthase: why two isoforms? *Am. J. Physiol.* 270, G393–G400
2. Arslan, A., and Zingg, H. H. (1996) Regulation of COX-2 gene expression in rat uterus in vivo and in vitro. *Prostaglandins* 52, 463–481
3. Tanaka, Y., Takahashi, M., Kawaguchi, M., and Amano, F. (1997) Delayed release of prostaglandins from arachidonic acid and kinetic changes in prostaglandin H synthase activity on the induction of prostaglandin H synthase-2 after lipopolysaccharide-treatment of RAW264.7 macrophage-like cells. *Biol. Pharm. Bull.* 20, 322–326
4. Sheng, H., Shao, J., Washington, M. K., and DuBois, R. N. (2001) Prostaglandin E2 increases growth and motility of colorectal carcinoma cells. *J. Biol. Chem.* 276, 18075–18081
5. Ben-Av, P., Crofford, L. J., Wilder, R. L., and Hla, T. (1995) Induction of vascular endothelial growth factor expression in synovial fibroblasts by prostaglandin E and interleukin-1: a potential mechanism for inflammatory angiogenesis. *FEBS Lett.* 372, 83–87
6. Tsuji, S., Kawano, S., Tsujii, M., Michida, T., Masuda, E., Gunawan, E. S., and Hori, M. (1998) Mucosal microcirculation and angiogenesis in gastrointestinal tract. *Nippon Rinsho* 56, 2247–2252
7. Sheng, H., Shao, J., Morrow, J. D., Beauchamp, R. D., and DuBois, R. N. (1998) Modulation of apoptosis and Bcl-2 expression by prostaglandin E2 in human colon cancer cells. *Cancer Res.* 58, 362–366
8. Kakiuchi, Y., Tsuji, S., Tsujii, M., Murata, H., Kawai, N., Yasumaru, M., Kimura, A., Komori, M., Irie, T., Miyoshi, E., et al. (2002) Cyclooxygenase-2 activity altered the cell-surface carbohydrate antigens on colon cancer cells and enhanced liver metastasis. *Cancer Res.* 62, 1567–1572
9. Tsuji, S., Tsujii, M., Kawano, S., and Hori, M. (2001) Cyclooxygenase-2 upregulation as a perigenetic change in carcinogenesis. *J. Exp. Clin. Cancer Res.* 20, 117–129
10. Sano, H., Kawahito, Y., Wilder, R. L., Hashiramoto, A., Mukai, S., Asai, K., Kimura, S., Kato, H., Kondo, M., and Hla, T. (1995) Expression of cyclooxygenase-1 and -2 in human colorectal cancer. *Cancer Res.* 55, 3785–3789
11. Murata, H., Kawano, S., Tsuji, S., Tsuji, M., Sawaoka, H., Kimura, Y., Shiozaki, H., and Hori, M. (1999) Cyclooxygenase-2 overexpression enhances lymphatic invasion and metastasis in human gastric carcinoma. *Am. J. Gastroenterol.* 94, 451–455
12. Xue, Y. W., Zhang, Q. F., Zhu, Z. B., Wang, Q., and Fu, S. B. (2003) Expression of cyclooxygenase-2 and clinicopathologic features in human gastric adenocarcinoma. *World J. Gastroenterol.* 9, 250–253
13. Achiwa, H., Yatabe, Y., Hida, T., Kuroishi, T., Kozaki, K., Nakamura, S., Ogawa, M., Sugiura, T., Mitsudomi, T., and Takahashi, T. (1999) Prognostic significance of elevated cyclooxygenase 2 expression in primary, resected lung adenocarcinomas. *Clin. Cancer Res.* 5, 1001–1005
14. Richards, R. G., and Almond, G. W. (1994) Lipopolysaccharide-induced increases in porcine serum cortisol and progesterone concentrations are not mediated solely by prostaglandin F2 alpha. *Inflammation* 18, 203–214
15. Davis, B. J., Lennard, D. E., Lee, C. A., Tiano, H. F., Morham, S. G., Wetsel, W. C., and Langenbach, R. (1999) Anovulation in cyclooxygenase-2-deficient mice is restored by prostaglandin E2 and interleukin-1beta. *Endocrinology* 140, 2685–2695
16. Caivano, M., and Cohen, P. (2000) Role of mitogen-activated protein kinase cascades in mediating lipopolysaccharide-stimulated induction of cyclooxygenase-2 and IL-1 beta in RAW264 macrophages. *J. Immunol.* 164, 3018–3025
17. Kirtikara, K., Raghow, R., Laulederkind, S. J., Goorha, S., Kanekura, T., and Ballou, L. R. (2000) Transcriptional regulation of cyclooxygenase-2 in the human microvascular endothelial cell line, HMEC-1: control by the combinatorial actions of AP2, NF-IL-6 and CRE elements. *Mol. Cell. Biochem.* 203, 41–51
18. Bamba, H., Ota, S., Kato, A., Adachi, A., Itoyama, S., and Matsuzaki, F. (1999) High expression of cyclooxygenase-2 in macrophages of human colonic adenoma. *Int. J. Cancer* 83, 470–475
19. Fiebich, B. L., Mueksch, B., Boehringer, M., and Hull, M. (2000) Interleukin-1beta induces cyclooxygenase-2 and prostaglandin E(2) synthesis in human neuroblastoma cells: involvement of p38 mitogen-activated protein kinase and nuclear factor-kappaB. *J. Neurochem.* 75, 2020–2028
20. Wadleigh, D. J., and Herschman, H. R. (1999) Transcriptional regulation of the cyclooxygenase-2 gene by diverse ligands in murine osteoblasts. *Biochem. Biophys. Res. Commun.* 264, 865–870
21. Crofford, L. J., Tan, B., McCarthy, C. J., and Hla, T. (1997) Involvement of nuclear factor kappa B in the regulation of cyclooxygenase-2 expression by interleukin-1 in rheumatoid synoviocytes. *Arthritis Rheum.* 40, 226–236
22. Inoue, H., Yokoyama, C., Hara, S., Tone, Y., and Tanabe, T. (1995) Transcriptional regulation of human prostaglandin-endoperoxide synthase-2 gene by lipopolysaccharide and phorbol ester in vascular endothelial cells. Involvement of both nuclear factor for interleukin-6 expression site and cAMP response element. *J. Biol. Chem.* 270, 24965–24971
23. Yoshida, S., Ono, M., Shono, T., Izumi, H., Ishibashi, T., Suzuki, H., and Kuwano, M. (1997) Involvement of interleukin-8, vascular endothelial growth factor, and basic fibroblast growth factor in tumor necrosis factor alpha-dependent angiogenesis. *Mol. Cell. Biol.* 17, 4015–4023
24. Torisu, H., Ono, M., Kiryu, H., Furue, M., Ohmoto, Y., Nakayama, J., Nishioka, Y., Sone, S., and Kuwano, M. (2000) Macrophage infiltration correlates with tumor stage and angiogenesis in human malignant melanoma: possible involvement of TNFalpha and IL-1alpha. *Int. J. Cancer* 85, 182–188
25. Ono, M., Torisu, H., Fukushi, J., Nishie, A., and Kuwano, M. (1999) Biological implications of macrophage infiltration in human tumor angiogenesis. *Cancer Chemother. Pharmacol.* 43, S69–S71
26. Kawai, S. (1998) Drug delivery system of anti-inflammatory and anti-rheumatic drugs. *Nippon Rinsho* 56, 782–787
27. Dequeker, J., Hawkey, C., Kahan, A., Steinbruck, K., Alegre, C., Baumelou, E., Begaud, B., Isomaki, H., Littlejohn, G., and Mau, J. (1998) Improvement in gastrointestinal tolerability of the selective cyclooxygenase (COX)-2 inhibitor, meloxicam, compared with piroxicam: results of the Safety and Efficacy Large-scale Evaluation of COX-inhibiting Therapies (SELECT) trial in osteoarthritis. *Br. J. Rheumatol.* 37, 946–951
28. Reddy, B. S., and Rao, C. V. (2000) Colon cancer: a role for cyclo-oxygenase-2-specific nonsteroidal anti-inflammatory drugs. *Drugs Aging* 16, 329–334
29. Giardiello, F. M., Hamilton, S. R., Krush, A. J., Piantadosi, S., Hylind, L. M., Celano, P., Booker, S. V., Robinson, C. R., and Offerhaus, G. J. (1993) Treatment of colonic and rectal adenomas with sulindac in familial adenomatous polyposis. *N. Engl. J. Med.* 328, 1313–1316
30. Oshima, M., Dinchuk, J. E., Kargman, S. L., Oshima, H., Hancock, B., Kwong, E., Trzaskos, J. M., Evans, J. F., and Taketo, M. M. (1996) Suppression of intestinal polyposis in Apc delta-716 knockout mice by inhibition of cyclooxygenase 2 (COX-2). *Cell* 87, 803–809
31. Oshima, M., Murai, N., Kargman, S., Arguello, M., Luk, P., Kwong, E., Taketo, M. M., and Evans, J. F. (2001) Chemoprevention of intestinal polyposis in the Apcdelta716 mouse by rofecoxib, a specific cyclooxygenase-2 inhibitor. *Cancer Res.* 61, 1733–1740
32. Sawaoka, H., Tsuji, S., Tsujii, M., Gunawan, E. S., Sasaki, Y., Kawano, S., and Hori, M. (1999) Cyclooxygenase inhibitors suppress angiogenesis and reduce tumor growth in vivo. *Lab. Invest.* 79, 1469–1477
33. Masferrer, J. L., Koki, A., and Seibert, K. (1999) COX-2 inhibitors. A new class of antiangiogenic agents. *Ann. N.Y. Acad. Sci.* 889, 84–86
34. Riendeau, D., Percival, M. D., Boyce, S., Brideau, C., Charleson, S., Cromlish, W., Ethier, D., Evans, J., Falgueyret, J. P., Ford-Hutchinson, A. W., et al. (1997) Biochemical and pharmacological profile of a tetrasubstituted furanone as a highly selective COX-2 inhibitor. *Br. J. Pharmacol.* 121, 105–117
35. Wakitani, K., Nanayama, T., Masaki, M., and Matsushita, M. (1998) Profile of JTE-522 as a human cyclooxygenase-2 inhibitor. *Jpn. J. Pharmacol.* 78, 365–371
36. Hirata, A., Ogawa, S., Kometani, T., Kuwano, T., Naito, S., Kuwano, M., and Ono, M. (2002) ZD1839 (Iressa) induces

antiangiogenic effects through inhibition of epidermal growth factor receptor tyrosine kinase. *Cancer Res.* 62, 2554–2560
37. Nakao, S., Kuwano, T., Ishibashi, T., Kuwano, M., and Ono, M. (2003) Synergistic effect of TNF-α in soluble VCAM-1-induced angiogenesis through α4 integrins. *J. Immunol.* 170, 5704–5711
38. Morham, S. G., Langenbach, R., Loftin, C. D., Tiano, H. F., Vouloumanos, N., Jennette, J. C., Mahler, J. F., Kluckman, K. D., Ledford, A., Lee, C. A., et al. (1995) Prostaglandin synthase 2 gene disruption causes severe renal pathology in the mouse. *Cell* 83, 473–482
39. Ogawa, S., Yoshida, S., Ono, M., Onoue, H., Ito, Y., Ishibashi, T., Inomata, H., and Kuwano, M. (1999) Induction of macrophage inflammatory protein-1α and vascular endothelial growth factor during inflammatory neovascularization in the mouse cornea. *Angiogenesis* 3, 327–334
40. Itokawa, T., Nokihara, H., Nishioka, Y., Sone, S., Iwamoto, Y., Yamada, Y., McMahon, G., Shibuya, M., Kuwano, M., Ono, M., et al. (2002) Antiangiogenic effect by SU5416 is partly attributable to inhibition of Flt-1 receptor signaling. *Mol. Cancer Ther.* 1, 295–302
41. Voronov, E., Shouval, D. S., Krelin, Y., Cagnano, E., Benharroch, D., Iwakura, Y., Dinarello, C. A., and Apte, R. N. (2003) IL-1 is required for tumor invasiveness and angiogenesis. *Proc. Natl. Acad. Sci. USA* 100, 2645–2650
42. Yano, S., Nokihara, H., Goto, H., Ogawa, H., Kanematsu, T., Miki, T., Uehara, H., Saijo, Y., Nukiwa, T., Sone, S., et al. (2003) Multifunctional interleukin-1β promotes metastasis of human lung cancer cells in SCID mice via enhanced expression of adhesion-, invasion- and angiogenesis-related molecules. *Cancer Sci.* 94, 244–252
43. Saijo, Y., Tanaka, M., Miki, M., Suzuki, T., Maemondo, M., Hong, X., Tazawa, R., Kikuchi, T., Matsushima, K., Nukiwa, T., et al. (2002) Proinflammatory cytokine IL-1β promotes tumor growth of Lewis lung carcinoma by induction of angiogenic factors: in vivo analysis of tumor-stromal interaction. *J. Immunol.* 169, 469–475
44. Salven, P., Hattori, K., Heissig, B., and Rafii, S. (2002) Interleukin-1α promotes angiogenesis in vivo via VEGFR-2 pathway by inducing inflammatory cell VEGF synthesis and secretion. *FASEB J.* 16, 1471–1473
45. Majima, M., Hayashi, I., Muramatsu, M., Katada, J., Yamashina, S., and Katori, M. (2000) Cyclo-oxygenase-2 enhances basic fibroblast growth factor-induced angiogenesis through induction of vascular endothelial growth factor in rat sponge implants. *Br. J. Pharmacol.* 130, 641–649
46. Cheng, T., Cao, W., Wen, R., Steinberg, R. H., and LaVail, M. M. (1998) Prostaglandin E2 induces vascular endothelial growth factor and basic fibroblast growth factor mRNA expression in cultured rat Muller cells. *Invest. Ophthalmol. Vis. Sci.* 39, 581–591
47. Graeber, J. E., Glaser, B. M., Setty, B. N., Jerdan, J. A., Walenga, R. W., and Stuart, M. J. (1990) 15-Hydroxyeicosatetraenoic acid stimulates migration of human retinal microvessel endothelium in vitro and neovascularization in vivo. *Prostaglandins* 39, 665–673
48. He, H., Venema, V. J., Gu, X., Venema, R. C., Marrero, M. B., and Caldwell, R. B. (1999) Vascular endothelial growth factor signals endothelial cell production of nitric oxide and prostacyclin through flk-1/KDR activation of c-Src. *J. Biol. Chem.* 274, 25130–25135
49. Daniel, T. O., Liu, H., Morrow, J. D., Crews, B. C., and Marnett, L. J. (1999) Thromboxane A2 is a mediator of cyclooxygenase-2-dependent endothelial migration and angiogenesis. *Cancer Res.* 59, 4574–4577
50. Coussens, L. M., and Werb, Z. (2002) Inflammation and cancer (review). *Nature (London)* 420, 860–867
51. Bol, D. K., Rowley, R. B., Ho, C. P., Pilz, B., Dell, J., Swerdel, M., Kiguchi, K., Muga, S., Klein, R., and Fischer, S. M. (2002) Cyclooxygenase-2 overexpression in the skin of transgenic mice results in suppression of tumor development. *Cancer Res.* 62, 2516–2521
52. Weidner, N., Semple, J. P., Welch, W. R., and Folkman, J. (1991) Tumor angiogenesis and metastasis–correlation in invasive breast carcinoma. *N. Engl. J. Med.* 324, 1–8
53. Zhang, X., Morham, S. G., Langenbach, R., and Young, D. A. (1999) Malignant transformation and antineoplastic actions of nonsteroidal antiinflammatory drugs (NSAIDs) on cyclooxygenase-null embryo fibroblasts. *J. Exp. Med.* 190, 451–459

Received for publication May 13, 2004.
Accepted for publication October 8, 2004.

Sensitivity to gefitinib (Iressa, ZD1839) in non-small cell lung cancer cell lines correlates with dependence on the epidermal growth factor (EGF) receptor/extracellular signal-regulated kinase 1/2 and EGF receptor/Akt pathway for proliferation

Mayumi Ono,[1] Akira Hirata,[1] Takuro Kometani,[1] Miho Miyagawa,[1] Shu-ichi Ueda,[1] Hisafumi Kinoshita,[2] Teruhiko Fujii,[3] and Michihiko Kuwano[3]

[1]Department of Medical Biochemistry, Graduate School of Medical Sciences, Kyushu University, Fukuoka, Japan and [2]Department of Surgery and [3]Research Center for Innovative Cancer Therapy of the 21st Century COE Program for Medical Science, Kurume University, Fukuoka, Japan

Abstract

Gefitinib (Iressa, ZD1839), a quinazoline tyrosine kinase inhibitor that targets the epidermal growth factor receptor (EGFR), is approved for patients with advanced non-small cell lung cancer (NSCLC) in several countries including Japan. However, the mechanism of drug sensitivity to gefitinib is not fully understood. In this study, we examined the molecular basis of sensitivity to gefitinib using nine human lung cancer cell lines derived from NSCLC. PC9 was the most sensitive to gefitinib of the nine NSCLC cell lines when assayed either by colony formation or MTS assays. The various cell lines expressed different levels of EGFR, HER2, HER3, and HER4, but there was no correlation between levels of EGFR and/or HER2 expression and drug sensitivity. Phosphorylation of EGFR, protein kinase B/AKT (Akt), and extracellular signal-regulated kinase (ERK) 1/2 was inhibited by much lower concentration of gefitinib in PC9 cells than in the other eight cell lines under exponential growing conditions. About 80% of cell surface EGFR in PC-9 was internalized within 10 min, whereas only about 30–50% of the cell surface EGFR was internalized in more drug-resistant cell lines in 15–60 min. The present study is the first to demonstrate that sensitivity to growth inhibition by gefitinib in NSCLC cell lines under basal growth condition is associated with dependence on Akt and ERK1/2 activation in response to EGFR signaling for survival and proliferation and also that drug sensitivity may be related to the extent of EGF-induced down-regulation of cell surface EGFR. [Mol Cancer Ther. 2004;3(4):465–472]

Received 8/29/03; revised 1/24/04; accepted 1/28/04.

Grant support: Grant-in-aid for cancer research from Ministry of Education, Culture, Sports, Science and Technology, and Ministry of Health, Labor and Welfare, Japan.

The costs of publication of this article were defrayed in part by the payment of page charges. This article must therefore be hereby marked advertisement in accordance with 18 U.S.C. Section 1734 solely to indicate this fact.

Note: Iressa is a trademark of the AstraZeneca group of companies.

Requests for Reprints: Mayumi Ono, Department of Medical Biochemistry, Graduate School of Medical Sciences, Kyushu University, 3-1-1 Maidashi, Higashi-ku, Fukuoka 812-8582, Japan. Phone: 81-92-642-6098; Fax: 81-92-642-6203. E-mail: mayumi@biochem1.med.kyushu-u.ac.jp

Introduction

Epidermal growth factor receptor (EGFR) is a prototypical member of the EGFR family that includes HER2/neu (ErbB2), HER3 (ErbB3), and HER4 (ErbB4) (1–3). EGFR responds to a number of growth factors such as EGF/TGFα and amphiregulin. This family of receptors plays critical roles in the operation of signaling networks affecting proliferation, migration, survival, adhesion, and differentiation (3). EGFR and/or HER2 are highly expressed in many tumors of epithelial origin, including cancers of lung, breast, head and neck, and bladder (4), and patients whose tumors express high levels of EGFR and/or HER2 have a poor prognosis (5). EGFR family members exist as monomers spanning the plasma membrane, and the monomeric receptors dimerize and become functionally active after binding to the appropriate soluble extracellular ligand. Signal transduction is mediated by a large family of EGF receptors and their ligands (6). Homo- and/or heterodimerization of EGFR activates a number of intracellular signal transducing elements such as phospholipase Cγ, phosphatidylinositol-3′-kinase, protein kinase B/AKT (Akt), a small G-protein (Ras), the Ras GTPase-activating protein, extracellular signal-regulated kinase (ERK) 1/2, Src family kinases, and STATs (7). We have reported that the angiogenesis signal also operates through the EGF-EGFR pathway (8).

Agents that target tyrosine kinase receptors may contribute to the treatment of malignancies that have relatively high levels of EGFR expression (9, 10). The tyrosine kinase inhibitor gefitinib (Iressa, ZD1839) is a synthetic anilinoquinazoline that targets EGFR (11); it has good oral bioavailability, and antitumor activity in a broad range of mouse xenograft models (9) and tumor cell lines (12). Clinically meaningful antitumor activity was observed in two phase II trials of gefitinib monotherapy in previously treated patients with advanced non-small cell lung cancer, NSCLC (IDEAL 1 and 2), and gefitinib is now approved in several countries including Japan, Australia, and the United States for the treatment of

advanced NSCLC (13, 14). Concerning the basis of the differential sensitivity of human malignancies to the antitumor effect of gefitinib, animal experiments with xenografts of human breast cancer and other epithelial tumor cell lines have shown that tumors that overexpress HER2 are the most sensitive to gefitinib (15, 16). However, it could be argued that EGFR and/or HER2 levels (17, 18), or phosphorylation of EGFR, or other EGF/TGFα signaling mechanisms (19) control the sensitivity of cancer cells to gefitinib. Naruse *et al.* (20) have reported that a human leukemic cell line resistant to phorbol ester was 400-fold more sensitive to gefitinib than its parent, suggesting that gefitinib is most effective against cancer cells with non-P-glycoprotein-mediated multidrug resistance. In the present study, we investigated the basis of sensitivity to gefitinib in nine human cancer cell lines derived from NSCLC and two epidermoid cancers as controls. We tested whether the expression levels of EGFR family receptors and Cbl, EGFR phosphorylation, activation of EGFR downstream effectors such as Akt, or ERK1/2, and EGF-induced down-regulation were correlated with sensitivity to gefitinib.

Materials and Methods

Materials

Gefitinib was provided by AstraZeneca (Macclesfield, United Kingdom) (8). Recombinant human EGF was purchased from PeproTech (London, United Kingdom). Anti-EGFR antibody and anti-phospho-EGFR antibody were purchased from Upstate Biotechnology (Lake Placid, NY). Antibodies to ERK1/2, phospho-ERK1/2, Akt, and phospho-Akt were from Cell Signaling Technology (Beverly, MA). ^{125}I-protein A was purchased from Amersham Biosciences Corp. (Piscataway, NJ).

Cell Culture

Cell lines H522, H322, H358 (American Type Culture Collection, Manassas, VA), QG56 and PC9 (Kyushu Cancer Center, Fukuoka, Japan), and LK2 (Japanese Collection of Research Bioresources, Tokyo, Japan) were cultured in RPMI supplemented with 10% fetal bovine serum (FBS). A549 (Japanese Collection of Research Bioresources) was cultured in MEM supplemented with 10% FBS and NEAA. EBC-1 (Japanese Collection of Research Bioresources) was cultured in MEM supplemented with 10% FBS, and human epidermoid carcinoma KB3-1 cells were cultured in MEM supplemented with 10% newborn calf serum. LK2/EGFR-2 and LK2/EGFR-5 cells were established after stable transfection with PIRE/EGFRShyg1 expression plasmids using Lipofectin 2000 Reagent (Invitrogen, Corp., Carlsbad, CA). They were cultured in RPMI supplemented with 10% FBS and 350 μg/ml hygromycin. Cells were maintained under standard cell culture conditions at 37°C and 5% CO_2 in a humid environment.

Colony Formation Assay

Cell survival was determined by plating 3–9 × 10^2 cells in 35-mm dishes. After 24 h, various concentrations of gefitinib were added, followed by incubation for 7–10 days at 37°C. Gefitinib was solubilized in DMSO and controls for all experiments were carried out by adding equivalent volumes of DMSO. Colonies were counted after Giemsa staining, as described previously (21). IC_{50} values and SDs were obtained from the best fit of the data to a sigmoidal curve using GraphPad software.

Cell Viability Assay

CellTiter-Glo Luminescent Cell Viability Assay Kit (Promega Corp., Madison, WI) was used to evaluate cytotoxicity in LK2 and its stable transfectants. One hundred microliter aliquots of exponentially growing cell suspension (3–5 × 10^3 cells) were seeded into 96-well plates, and 24 h later, various concentrations of gefitinib were added. After incubation for 72 h at 37°C, 100 μl of CellTiter-Glo reagent were added and luminescence measured with a multilabel counter (Wallac, Tokyo, Japan). Each experiment was performed in three replicate wells for each drug concentration.

MTS Assay

A CellTiter 96^R AQ_{ueous} One Solution Cell Proliferation Assay Kit (Promega) was used to evaluate cytotoxicity. One hundred microliter samples of an exponentially growing cell suspension (5–8 × 10^3 cells) were seeded into a 96-well microtiter plate, and various concentrations of gefitinib were added. After incubation for 72 h at 37°C, 20 μl of CellTiter 96^R AQ_{ueous} One Solution were added to each well and the plates were incubated for a further 4 h at 37°C. Absorbance was measured at 490 nm with a 96-well plate reader. Each experiment was performed in three replicate wells for each drug concentration. The IC_{50} value is defined as the concentration needed for a 50% reduction in absorbance calculated from the survival curves.

Western Blot Analysis

To examine EGF-stimulated phosphorylation of proteins, confluent tumor cells were cultured in serum-free medium for 24 h. The cells were pretreated with gefitinib at concentrations up to 5 μM for 3 h before exposure to 20 ng/ml EGF for 15 min at 37°C. To examine phosphorylation under basal conditions, subconfluent tumor cells cultured in medium supplemented with 10% FBS were incubated with various concentrations of gefitinib for 3 h at 37°C. The cells were then rinsed with ice-cold PBS and lysed in Triton X-100 buffer. The cell lysates were subjected to SDS-PAGE and transferred to Immobilon membranes (Millipore, Bedford, MA). After transfer, the blots were incubated with blocking solution and probed with various antibodies followed by washing. Proteins were visualized with HRP-conjugated secondary antibodies followed by enhanced chemiluminescence (ECL, Amersham).

EGFR Down-Regulation

Confluent cells in 24-well dishes were incubated with or without 500 ng/ml of EGF for up to 1 h at 37°C in binding medium (0.1% bovine serum albumin in RPMI). Then the cells were washed twice with PBS to remove EGF and incubated for 1 h at 4°C with a 1:100 dilution of anti-EGFR monoclonal antibody recognizing the extracellular domain of human EGFR. After washing, the cells were incubated with 20,000 cpm/ml of ^{125}I-protein A (0.5 ng/ml) for 1 h at 4°C in binding medium. The cells were again washed and

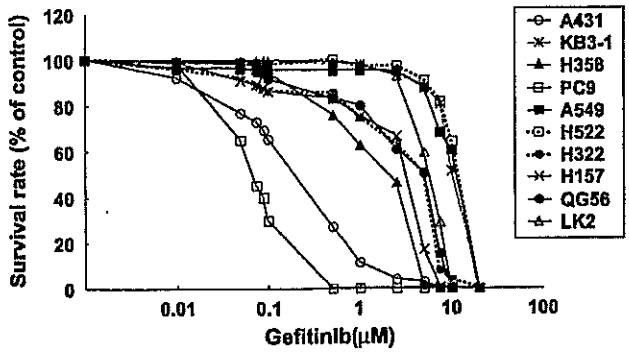

Figure 1. Dose-response curves of 10 human cancer cell lines, including 8 NSCLC lines and 2 epidermoid cancer lines, to gefitinib. Cell survival was determined by colony formation assay in the absence or presence of various doses of gefitinib. Number of colonies after incubation for 7 days with or without gefitinib were presented when normalized by colony numbers in the average of duplicate dishes. The IC_{50} for each cell line was presented from dose-response curves. Almost all cell lines except one line named EBC-1 were found to form colonies.

lysed with 1 N NaOH to determine the fraction of radioactivity (22). The linear regression coefficient of the dependence of this ratio on time represents the specific rate constant for down-regulation (K_e).

Results

Sensitivity to Gefitinib in NSCLC and Epidermoid Carcinoma Cell Lines

We first compared the effect of gefitinib on a panel of nine NSCLC cell lines, and two epidermoid carcinoma cell lines as controls, by both colony formation and MTS assay. Eight of the nine NSCLC cell lines and the two epidermoid cancer cell lines showed considerable resistance to gefitinib. Dose-response curves to gefitinib for 10 of the 11 human cancer cell lines assessed by the colony formation assay are presented in Fig. 1, and IC_{50} values for the 11 cell lines are given in Table 1. The seven NSCLC lines, A549, H522, H322, H358, H157, QG56, and LK2 showed 100- to 200-fold greater resistance to gefitinib than PC9 cells; the latter had an IC_{50} of 0.06 μM. The drug sensitivity of all 11 human cancer cell lines was also examined by MTS assay, and the IC_{50} values are also presented in Table 1. By the MTS assay, the IC_{50} of PC9 was 4 μM, and A549, H522, H322, H358, EBC-1, H157, QG56, and LK2 had 5- to 10-fold greater resistance to gefitinib (Table 1). In the colony formation assay, one of the epidermoid carcinoma cell lines, KB3-1, showed 25-fold higher resistance to gefitinib than the other cell line, A431, which had an IC_{50} of 0.4 μM (Fig. 1 and Table 1). When assayed by the MTS assay, the KB3-1 cells showed only a 2-fold higher resistance to gefitinib than the A431 cells (Table 1). Although the relative resistance of the other NSCLC and epidermoid cell lines compared with PC9 and A431 cells was much less when assayed by MTS than by colony formation, both assays concurred in indicating that the PC9 and A431 cells were more sensitive to gefitinib than the other cell lines examined in this study.

Expression of EGFR and Its Family of Receptor Proteins, HER2, HER3, and HER4

We examined expression of EGFR, HER2, HER3, and HER4 in all the cell lines used in this study by Western blot analysis. Expression of EGFR and its family members, HER2, HER3, and HER4, in the NSCLC cell lines varied considerably (Fig. 2). The level of expression of the receptors in each of the NSCLC and epidermoid cancer cell line is given in Fig. 2 relative to expression levels in the drug-sensitive lines PC9 and A431, respectively. One of the

Table 1. Cell lines employed in this study, sensitivities to gefitinib, and EGF-induced stimulation of EGFR, Akt, and ERK1/2

Cell Lines	Origin	IC_{50} (μM)[a]		Fold Stimulation by EGF[b]		
		Colony Formation	MTS	EGFR	Akt	ERK1/2
PC9	Human NSCLC (Adenocarcinoma)	0.06 (1.0)	4 (1.0)	1.6	4.0	2.9
A549	Human NSCLC (Adenocarcinoma)	13 (217)	21 (5.3)	3.5	11.1	15.6
H522	Human NSCLC (Adenocarcinoma)	13 (217)	20 (5.0)	2.4	1.9	4.5
H322	Human NSCLC (Adenocarcinoma)	6.8 (113)	27 (6.8)	6.6	2.8	1.7
H358	Human NSCLC (Adenocarcinoma)	2.0 (33)	12 (3.0)	3.2	2.1	8.8
EBC-1	Human NSCLC (Squamous cell carcinoma)	ND[c]	21 (5.3)	1.3	1.1	1.4
H157	Human NSCLC (Squamous cell carcinoma)	12 (200)	30 (7.5)	125	4.1	2.3
QG56	Human NSCLC (Squamous cell carcinoma)	7.8 (130)	42 (10.5)	1.5	3.8	12.7
LK2	Human NSCLC (Squamous cell carcinoma)	8.0 (133)	20 (5.0)	nd[d]	3.3	3.2
A431	Human epidermoid carcinoma	0.4 (1.0)	10 (1.0)	1.6	1.8	8.7
KB3-1	Human epidermoid carcinoma	10 (25)	15 (1.5)	31.3	4.2	6.9

[a]Drug sensitivity of nine human non-small lung cancer cell lines and two epidermoid cancer cell lines to gefitinib was assayed by both colony formation and MTS. IC_{50} value for each cell line is presented from two independent assays, and relative activity is presented in parentheses when normalized by IC_{50} for PC9 cells.
[b]The fold stimulation by EGF of EGFR, Akt, and ERK 1/2 is presented for each cell line when normalized by untreated control in the absence of EGF (see Fig. 4).
[c]ND, not determined because of poor colony-forming ability of the cell line.
[d]nd, not detected because of poor phosphorylation.

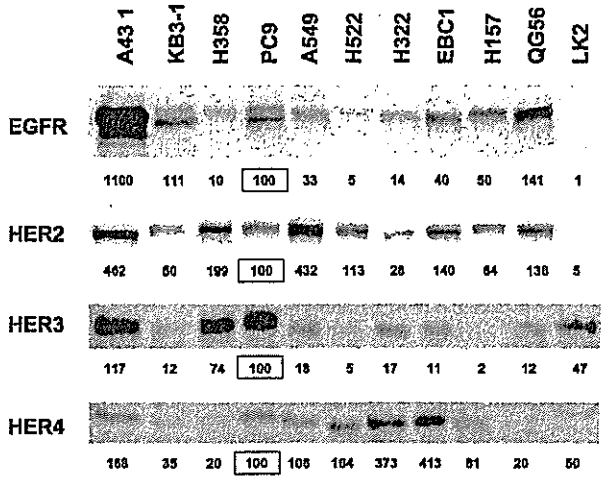

Figure 2. Protein expression of four EGFR family members, EGFR, HER2, HER3, and HER4, in nine NSCLC lines and two epidermoid carcinoma cell lines. Cellular protein levels of four EGFR family proteins were determined by Western blot analysis using specific antibodies. Each lane was analyzed with 100 μg protein of cell lysates from each cell line. Relative expression protein levels for NSCLC and epidermoid cancer cell line are presented when protein level of each EGFR family for PC9 and A431 is presented as 100%.

NSCLC cells, LK2 that expressed almost no detectable EGFR and HER2, was relatively resistant to gefitinib. On the other hand, QG56 cells that expressed more EGFR than PC9 cells were much less sensitive than the latter to gefitinib (Table 1). Expression of the four family members, EGFR, HER2, HER3, and HER4, varied among the NSCLC cell lines. Of two epidermoid cancer cell lines, gefitinib-resistant KB3-1 cells had only 10% of the EGFR level of A431 cells. In contrast, five of the NSCLC cell lines (H358, A549, H522, EBC1, QG56) had more HER2, while four NSCLC cell lines had lower levels of HER3 than PC9. KB3-1 cells had 10–20% of the EGFR, HER2, HER3, and HER4 of A431 cells (Fig. 2). Thus, expression of the four EGFR family members is not correlated with the cytotoxicity of gefitinib. We next examined if increasing the expression of EGFR in LK2 cells, which expressed very low levels, if any, of EGFR (see Fig. 2) would render them sensitive to gefitinib. Two EGFR transfectants (LK2/EGFR-2 and LK2/EGFR-5) were isolated by introducing cDNA of human EGFR into the LK2 cells. These EGFR transfectants had much higher EGFR levels than their parent, or mock transformed LK2 cells (Fig. 3A). However, their sensitivity to gefitinib was similar to that of the parent strain when assayed by the cell viability assay (Fig. 3B).

Effect of Gefitinib on Phosphorylation of EGFR, Akt, and ERK1/2

EGF/TGFα causes phosphorylation of EGFR by its tyrosine kinase activity, and leads to activation of a number of downstream cytoplasmic signaling molecules (6). We first examined the effect of gefitinib on phosphorylation of EGFR, Akt, and ERK1/2 in response to EGF (EGF-induced phosphorylation) in the cell lines used in this study.

Figure 4 shows the inhibitory effect of gefitinib on EGF-induced autophosphorylation of EGFR, and phophorylation of Akt and ERK1/2 in three of the NSCLC cell lines. EGF stimulated EGFR autophosphorylation and activation of Akt and ERK1/2 in PC9 (A), A549 (B), and QG56 (C) cells, and activation was blocked to different extents by gefitinib. Table 2 presents IC_{50} (μM) values for EGF-induced autophosphorylation of EGFR, and for phosphorylation of Akt and ERK1/2. IC_{50} gefitinib doses for EGF-induced autophosphorylation of EGFR were similar in all the NSCLC cell lines including PC9 although the drug-resistant lines EBC-1 and H157 had 2.7- and 0.2-fold higher IC_{50} (μM) values. EGF-induced Akt phosphorylation in four of the NSCLC cell lines was 10-fold or more resistant to gefitinib than in PC9 cells while the other cell lines showed similar IC_{50} values to PC9. ERK1/2 phosphorylation was highly

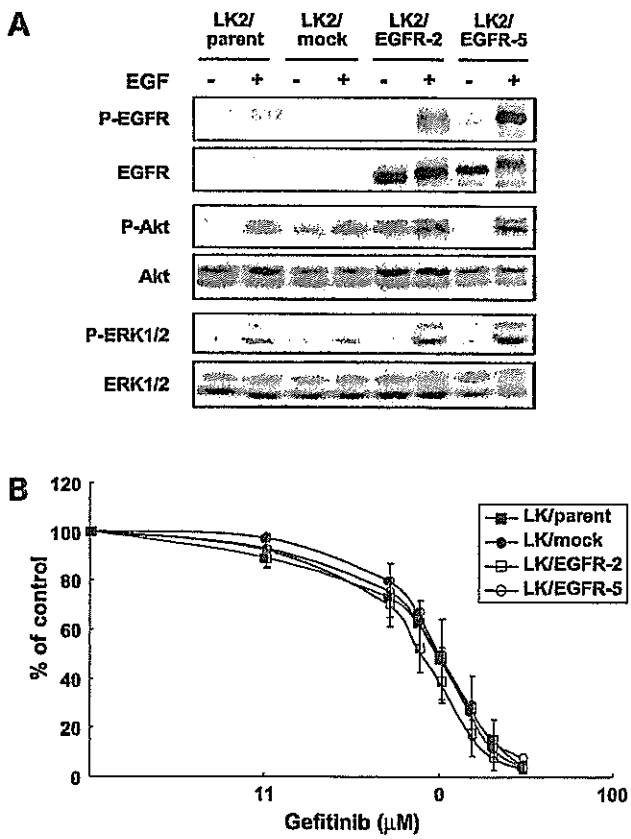

Figure 3. Protein expression of EGFR in LK2 and its two EGFR transfectants (LK2/EGFR2 does not alter sensitivity to gefitinib in LK2 cells). **A**, comparison of EGFR, Akt, and ERK1/2 protein expression levels and phosphorylation of EGFR, Akt, and ERK1/2 with or without EGF in a subclone of LK2 cells transfected with EGFR or mock vector. Serum-starved cells were treated with 20 ng/ml EGF for 10 min. Protein extracts were resolved by 7.5% SDS-PAGE and probed with either antibody. Immunoreactive proteins were visualized by enhanced chemiluminescence. **B**, dose-response curves of a subclone of LK2 cells transfected with EGFR or mock vector to gefitinib. Sensitivity to gefitinib was determined by cell viability assay in the absence or presence of various doses of gefitinib. The number of viable cells was calculated at 72 h and graphed as percentage of untreated cells. *Points*, average of triplicate dishes; *bars*, SD.

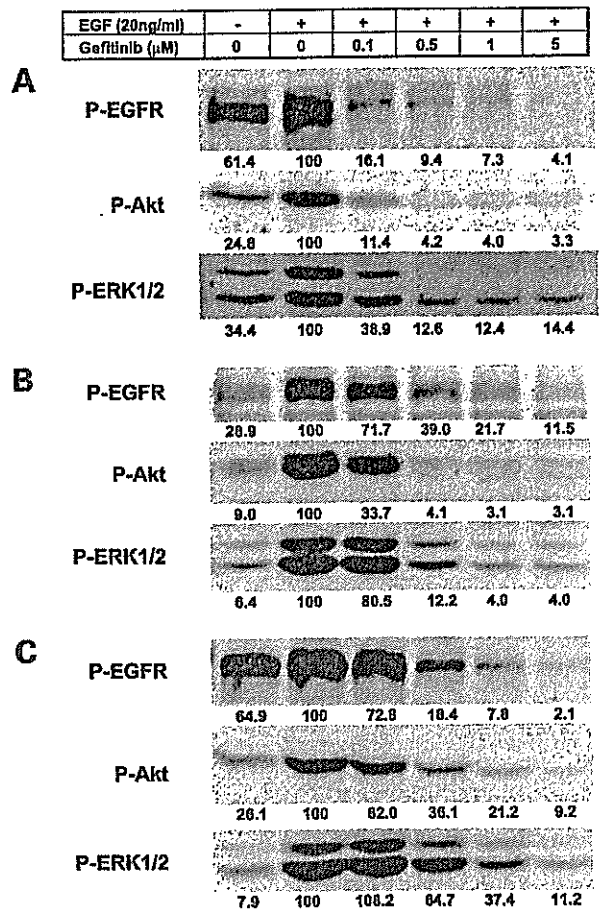

Figure 4. Dose-dependent inhibition of EGF-induced EGFR autophosphorylation, Akt and ER1/2 phosphorylation in three human cancer cells. Serum-starved cancer cells were treated for 3 h with the indicated concentrations of gefitinib, followed by the addition of EGF (20 ng/ml) for 15 min. Protein extracts were resolved by 7.5% SDS-PAGE and probed with either antibody. Immunoreactive proteins were visualized by enhanced chemiluminescence. **A**, PC9 cells; **B**, A549 cells; and **C**, QG56 cells.

resistant to gefitinib in most of the NSCLC cell lines, while the remaining three were only weakly resistant (1.1- to 3.1-fold). The two epidermoid carcinoma cell lines, A431 and KB3-1, showed similar IC_{50} values for gefitinib with respect to EGFR, Akt, and ERK1/2 phosphorylation (Table 2).

Figure 5 presents the effects of gefitinib on phosphorylation of EGFR, Akt, and ERK1/2 in three cell lines under basal growth condition in the presence of 10% serum. EGFR autophosphorylation and activation of Akt and ERK1/2 in PC9 (A), A549 (B), and QG56 (C) cells were inhibited to different extents. In PC9 cells, EGFR autophosphorylation as well as Akt and ERK1/2 activation were almost completely blocked by 0.1 μM gefitinib (Fig. 5A). By contrast, in the other two cell lines, A549 and QG56, there was only slight if any inhibition of the activation of Akt and ERK1/2 despite the fact that EGFR phosphorylation was completely inhibited at 0.5–5 μM (Fig. 5, B and C). Under basal growth condition, all three processes, EGFR autophosphorylation and activation of Akt and ERK1/2 were the most susceptible to inhibition by gefitinib in PC9 cells. The IC_{50} for EGFR autophosphorylation was only 0.07 μM in PC9 while the IC_{50} values in the other cell lines were about 4-fold or more higher. KB3-1 cells also showed a 3-fold higher IC_{50} for EGFR autophosphorylation than the A431 cells. Gefitinib inhibited Akt activation under basal growth condition with an IC_{50} of 0.08 μM in PC9, whereas the IC_{50} values for QG56 and the other seven cell lines were 4- to 125-fold higher. The dose of gefitinib to inhibit ERK1/2 activation in PC9 cells under basal growth condition was almost 200-fold lower than that required to inhibit the other seven NSCLC cell lines (Table 2). The IC_{50} value for ERK1/2 activation in H358 cells was about 3-fold higher than in PC9 cells, while the IC_{50} values for both Akt and ERK1/2 phosphorylation in KB3-1 were much higher than in the drug-sensitive A431 cells (Table 2).

Table 2. Inhibition by gefitinib of EGF-induced and basal phosphorylation of EGFR, Akt, and ERK1/2 in nine NSCLC and two epidermoid carcinoma cells

Cell Lines	EGF-Induced (IC_{50}, μM)[a]			Basal Condition (IC_{50}, μM)		
	P-EGFR	P-Akt	P-ERK1/2	P-EGFR	P-Akt	P-ERK1/2
PC9	0.30 (1.0)	0.05 (1.0)	0.07 (1.0)	0.07 (1.0)	0.08 (1.0)	0.03 (1.0)
A549	0.22 (0.7)	0.06 (1.2)	0.22 (3.1)	0.25 (3.6)	5< (63<)	5< (167<)
H522	0.30 (1.0)	0.50 (10)	0.40 (5.7)	0.50 (7.1)	5 (63)	5< (167<)
H322	0.43 (1.4)	0.13 (2.0)	5< (71<)	0.35 (5.0)	5< (63<)	5< (167<)
H358	0.40 (1.3)	0.13 (2.0)	0.75 (11)	5 (71)	5< (63<)	0.1 (3.3)
EBC-1	0.80 (2.7)	5< (100<)	5< (71<)	5 (71)	10< (125<)	10< (333<)
H157	0.06 (0.2)	0.07 (1.4)	0.13 (1.9)	0.7 (10)	5 (63)	5< (167<)
QG56	0.20 (0.7)	0.90 (18)	2.20 (31)	0.3 (4.3)	0.35 (4.4)	5< (167<)
LK2	nd[b]	0.50 (10)	0.08 (1.1)	nd	10< (125<)	10< (333<)
A431	0.04 (1.0)	0.10 (1.0)	0.04 (1.0)	0.05 (1.0)	0.5 (1.0)	0.1 (1.0)
KB3-1	0.04 (1.0)	0.12 (1.2)	0.05 (1.3)	0.13 (2.6)	5 (10)	5< (50<)

[a] IC_{50} values were obtained from 50% inhibitory doses of gefitinib on phosphorylation of EGFR, Akt, and ERK1/2 under EGF-stimulated or basal (10% serum) culture condition as presented in Fig. 2. The relative activity for IC_{50} of each cell line is presented in parentheses when normalized by the IC_{50} value in PC9 and A431, respectively.
[b] nd, not detected because of poor phosphorylation.

EGF-Induced EGFR Down-Regulation and Expression of Cbl Protein

Cell surface EGFR is internalized during EGF/TGFα-driven receptor recycling in exponentially growing cells. We compared the rates of EGF-induced internalization of EGFR in the cell lines expressing relatively high amounts of EGFR (Fig. 6). After exposure to EGF, EGFR was rapidly down-regulated from the cell surface, and we found that 80% and 60% of the cell surface EGFR was internalized within 15 min in PC9 and A431 cells, respectively. In contrast, there was only 30–50% loss of cell surface EGFR 15–40 min after EGF stimulation in EBC-1, A549, and QG56 cells. Sixty percent to 80% of the EGFR molecules thus appeared to be rapidly internalized from the cell surface in gefitinib-sensitive cells, whereas much fewer EGFR molecules were internalized in the resistant cells and internalization was slower.

Cbl is a key protein limiting the initial step of EGFR endocytosis (6), and the EGFR signaling complex is degraded in a coordinate manner with Cbl after interacting with EGF (23). We examined expression of Cbl protein in the nine NSCLC cell lines and two epidermoid carcinoma cell lines (Fig. 7). Almost all the cell lines differed in their expression of Cbl with EBC-1 and QG56 cells expressing considerably less Cbl than the other cell lines. The relative expression levels of Cbl protein in both the NSCLC and epidermoid cancer cell lines are presented in Fig. 7. Cbl expression appears not to be correlated with either the rate of EGF-induced down-regulation (see Fig. 6) or sensitivity to gefitinib (Table 1).

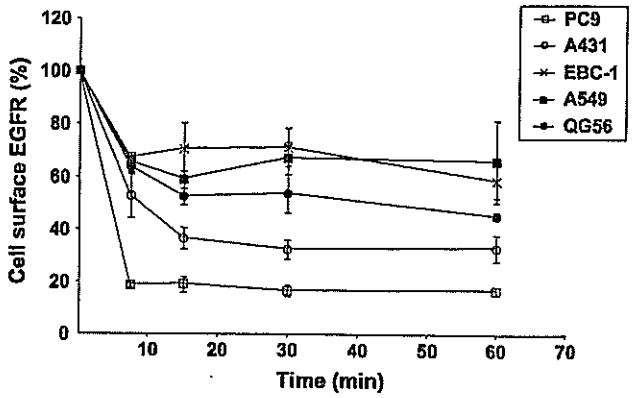

Figure 6. Time kinetics for EGF-induced down-regulation of EGFR. All cell lines (*PC9, EBC-1, A549, QG56, A431*) were further incubated with 500 ng/ml EGF at 37°C for the indicated periods. Then cells were incubated for 1 h at 4°C with a monoclonal antibody against human EGF receptor which specifically recognizes extracellular domain of EGFR and for another 1 h with ^{125}I-protein A. Relative amount of ^{125}I-protein A bound to the EGFR antibody is plotted and cell surface EGFR was determined by ^{125}I-protein A (see Materials and Methods; Ref. 22). *Points*, average of triplicate dishes; *bars*, SD.

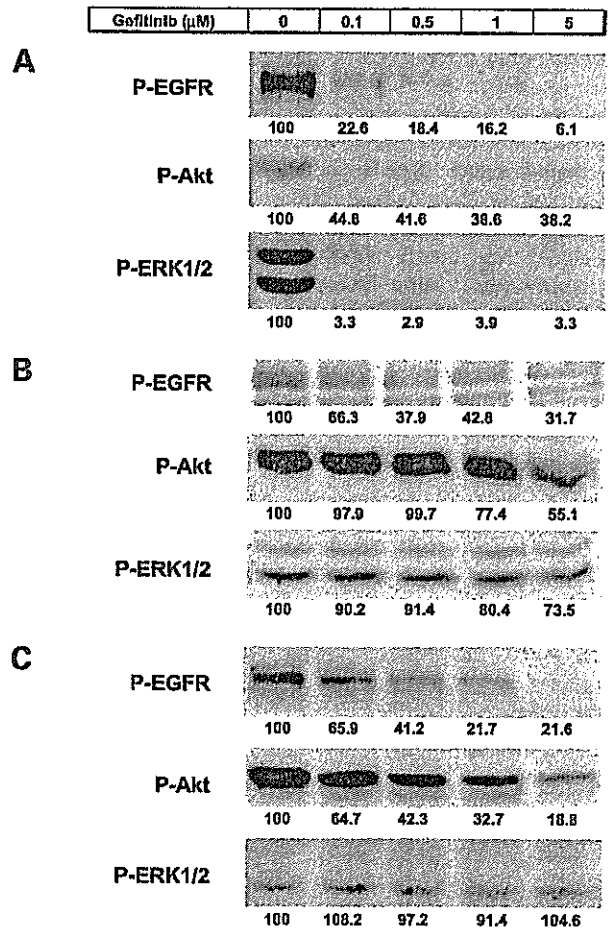

Figure 5. Dose-dependent inhibition by gefitinib of EGFR, Akt and ERK1/2 phosphorylation under basal growth conditions in three human cancer cell lines. Exponentially growing cells in 10% serum medium were pretreated for 3 h with the indicated concentrations of gefitinib. Protein extracts were resolved by 7.5% SDS-PAGE and probed with either antibody. EGFR, Akt, and ERK1/2 activity was determined using each corresponding anti-phospho antibody. Immunoreactive proteins were visualized by enhanced chemiluminescence. A, PC9 cells; B, A549 cells; and C, QG56 cells.

Discussion

Of the nine NSCLC cell lines, PC9, derived from an adenocarcinoma, was the most sensitive to the EGFR-targeting agent, gefitinib, and of the two epidermoid cancer cell lines, A431 was more sensitive to gefitinib than KB3-1. The sensitivity of PC9 was similar to that of A431. All these cell lines except LK2 expressed some, although variable, levels of EGFR, HER2, HER3, and HER4. EGFR expression in PC9 was similar to that of some of resistant NSCLC cell

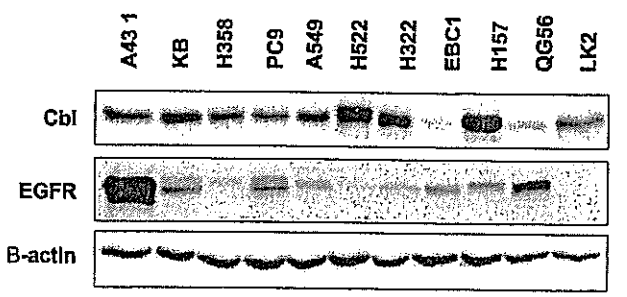

Figure 7. Expression of Cbl and EGFR protein in nine NSCLC cell lines and two epidermoid carcinoma cell lines. Protein levels of Cbl, EGFR, and β-actin determined by Western blot analysis using 100 μg protein of cell lysate of each cell line from NSCLC and EC lines are presented when PC9 (NSCLC) and A431 (EC) are respectively normalized as 100%.

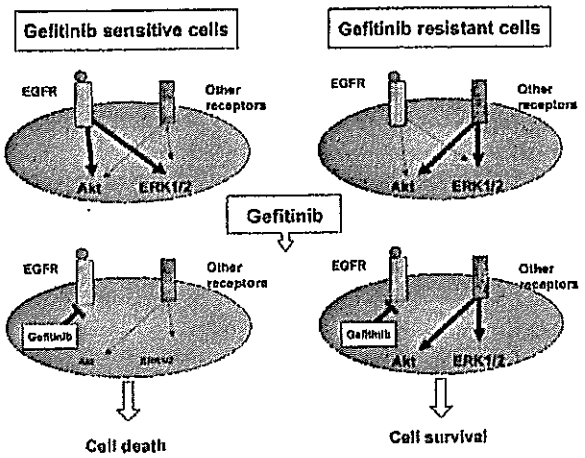

Figure 8. A model of how drug sensitivity to gefitinib is controlled in NSCLC and EC. From our present study, in gefitinib-sensitive cell lines (PC9 and A431), only EGFR-driven signaling following activation of both Akt and ERK1/2 was dominant for survival. On the other hand, in gefitinib-resistant cells, EGFR is not a survival factor and other factor or receptor-driven cell survival following activation of downstream signaling effectors was dominant. Therefore, cells, the survival and apoptosis of which are totally dependent on EGFR signaling, are highly susceptible to gefitinib.

lines. We also observed no apparent difference in sensitivity to gefitinib between LK2 and two EGFR derivatives (LK2/EGFR-2 and LK2/EGFR-5), suggesting that it is unlikely that the level of EGFR expression is directly associated with sensitivity to gefitinib. A related study by Moasser *et al.* (15) reported that tumors overexpressing HER2 were highly sensitive to gefitinib. However, our data show that HER2 expression was much higher in five of the drug-resistant NSCLC lines than in PC9 (Fig. 2). The expression of two other EGFR family members, HER3 and HER4, also varied among the nine NSCLC lines, suggesting again that it is also unlikely that cellular HER3 and HER4 levels are related to sensitivity to gefitinib. In the two epidermoid cancer lines, expression of the four EGFR family members was much higher in the gefitinib-sensitive A431 cells than in the KB3-1 cells. However, this correlation is not convincing because we only compared two cell lines.

Stimulation with EGF/TGFα and other ligands activates Akt, ERK1/2, and other molecules, and such EGFR signaling controls cell migration, adhesion, apoptosis, cell cycle progression, growth, and angiogenesis (3). In our present study, we examined the effect of gefitinib on EGFR autophosphorylation and the downstream signaling by ERK1/2 and Akt under both EGF-induced and basal growth condition (Table 2). When the cells were stimulated with EGF, exposure to gefitinib blocked EGFR autophosphorylation at similar concentrations in all NSCLC cell lines including PC9. Inhibition of EGF-induced phosphorylation of ERK1/2 required higher doses of gefitinib in all the other NSCLC lines than in PC9 (Table 2). Treatment with gefitinib also inhibited EGF-induced Akt phosphorylation at similar doses in five of eight NSCLC cell lines including PC9 cells. Therefore, EGF-induced EGFR autophosphorylation and Akt activation do not appear to be related to levels of sensitivity to gefitinib.

Under basal growth conditions in the presence of 10% serum, inhibition of EGFR autophosphorylation in seven of the NSCLC cell lines required 4-fold (or higher) levels of gefitinib than PC9 (Table 2). To our surprise, activation of both Akt and ERK1/2 in almost all the NSCLC lines was found to be much less susceptible to the inhibitory effect of gefitinib under basal growth condition than in the drug-sensitive PC9 cells (Table 2). The activation of EGFR, Akt, and ERK1/2 in A431 cells was also highly sensitive to inhibition in comparison with KB3-1. Taken together, these findings indicate that under basal growth condition, high sensitivity to gefitinib in NSCLC and epidermoid cancer lines is closely correlated with dependence on Akt and ERK1/2 activation in response to EGFR signaling for survival and proliferation (see Fig. 8). Consistent with this notion, Barnes *et al.* (24) have reported that gefitinib inhibited EGFR and mitogen-activated protein kinase (MAPK) activation efficiently in exponentially growing cutaneous carcinoma cells.

We also observed an apparent difference in EGF-induced down-regulation of cell surface EGFR between drug-sensitive PC9 or A431 cells and drug-resistant EBC-1, A549, QG56, and KB3-1 cells (see Fig. 6). Almost all cell surface EGFR molecules were rapidly internalized in PC9 or A431 cells when only 30–50% of the cell surface EGFR molecules were slowly internalized in gefitinib-resistant cell lines. EGFR molecules in the sensitive cell lines seem to be highly susceptible to EGF stimulation with the result that they transduce the signals more effectively than the drug-resistant cells. We also examined expression of Cbl protein (Fig. 7). Cbl is a key protein affecting receptor internalization in general. However, there was no correlation between level of Cbl protein and EGF-induced down-regulation of EGFR.

In conclusion, one NSCLC cell line, PC9, of the nine strains examined was especially sensitive to the effect of gefitinib. This sensitivity appears to follow from the fact that this cell line is much more dependent than the others on the EGF receptor/ERK1/2 and Akt pathway for its survival and proliferation (see Fig. 8). The sensitivity of the EGFR pathway could be useful for predicting the likely effectiveness of gefitinib in NSCLC patients. Further analysis of other signaling processes in addition to EGFR phosphorylation are called for using clinical specimens.

References

1. Mendlsohn J, Baserga J. The EGF receptor family as targets for cancer therapy. Oncogene, 2000;19:6550–65.

2. de Bono JS, Rowinsky EK. The ErbB receptor family: a therapeutic target for cancer. Trends Mol Med, 2002;8:19–26.

3. Woodburn JR. The epidermal growth factor receptor and its inhibition in cancer therapy. Pharmacol Ther, 1999;82:241–50.

4. Arteaga CL. Epidermal growth factor receptor dependence in human tumors: more than just expression? Oncologist, 2002;7:31–9.

5. Brabender J, Danenberg KD, Metzger R, et al. Epidermal growth factor receptor and HER2-neu mRNA expression in non-small cell lung cancer is correlated with survival. Clin Cancer Res, 2001;7:1850–5.

6. Yarden Y. The EGFR family and its ligands in human cancer signaling mechanisms and therapeutic opportunities. Eur J Cancer, 2001;37: 3–8.

7. Raymond E, Faivre S, Armand JP. Epidermal growth factor receptor tyrosine kinase as a target for anticancer therapy. Drugs, 2000;60:15–23; discussion 41–2.

8. Hirata A, Ogawa S, Kometani T, et al. ZD1839 (Iressa) induces antiangiogenic effects through inhibition of epidermal growth factor receptor tyrosine kinase. Cancer Res, 2002;62:2554–60.

9. Sirotnak FM, Zakowski MF, Miller VA, Scher HI, Kris MG. Efficacy of cytotoxic agents against human tumor xenografts is markedly enhanced by coadministration of ZD1839 (Iressa), a inhibitor of EGFR tyrosine kinase. Clin Cancer Res, 2000;6:4885–92.

10. Slichenmyer WJ, Fry DW. Anticancer therapy targeting the erbB family of receptor tyrosine kinases. Semin Oncol, 2001;28:67–79.

11. Baselga J, Averbuch SD. ZD1839 (Iressa) as an anticancer agent. Drugs, 2000;60:33–40; discussion 41–2.

12. Ciardiello FI, Caputo R, Bianco R, et al. Antitumor effect and potentiation of cytotoxic drug activity in human cancer cells by ZD1839 (Iressa), an epidermal growth factor receptor-selective tyrosine kinase inhibitor. Clin Cancer Res, 2000;6:2053–63.

13. Fukuoka M, Yano S, Giaccone G, et al. Multi-institutional randomized phase II trial of gefitinib for previously treated patients with advanced non-small-cell lung cancer. J Clin Oncol, 2003;21:2237–46.

14. Kris MG, Natale RB, Herbest RS, et al. A phase II trial of ZD1839 ('Iressa') in advanced non-small cell lung cancer (NSCLC) patients who had failed platinum- and docetaxel-based regimens (IDEAL 2). Proc Am Soc Clin Oncol, 2002;21:292a #1166.

15. Moasser MM, Basso A, Averbuch SD, Rosen N. The tyrosine kinase inhibitor ZD1839 ('Iressa') inhibits HER2-driven signaling and suppresses the growth of HER2-overexpressing tumor cells. Cancer Res, 2001;61:7184–8.

16. Moulder SL, Yakes FM, Muthuswamy SK, Bianco R, Simpson JF, Arteaga CL. Epidermal growth factor receptor (HER1) tyrosine kinase inhibitor ZD1839 (Iressa) inhibits HER2/neu (erbB2)-overexpressing breast cancer cells *in vitro* and *in vivo*. Cancer Res, 2001;61:8887–95.

17. Anderson NG, Ahmad T, Chan K, Dobson R, Bundred NJ. ZD1839 (Iressa), a novel epidermal growth factor receptor (EGFR) tyrosine kinase inhibitor, potently inhibits the growth of EGFR-positive cancer cell lines with or without erbB2 overexpression. Int J Cancer, 2001;94:774–82.

18. Bishop PC, Myers T, Robey R, et al. Differential sensitivity of cancer cells to inhibitors of the epidermal growth factor receptor family. Oncogene, 2002;21:119–27.

19. Magne N, Fischel JL, Dubreuil A, et al. Influence of epidermal growth factor receptor (EGFR), p53 and intrinsic MAP kinase pathway status of tumor cells on the antiproliferative effect of ZD1839 (Iressa). Br J Cancer, 2002;86:1518–23.

20. Naruse I, Ohmori T, Ao Y, et al. Antitumor activity of the selective epidermal growth factor receptor-tyrosine kinase inhibitor (EGFR-TKI) Iressa (ZD1839) in an EGFR-expressing multidrug-resistant cell line *in vitro* and *in vivo*. Int J Cancer, 2002;98:310–5.

21. Koike K, Kawabe T, Tanaka T, et al. A canalicular multispecific organic anion transporter (cMOAT) antisense cDNA enhances drug sensitivity in human hepatic cancer cells. Cancer Res, 1997;57:5475–9.

22. Ono M, Nakayama Y, Gopas JG, Kung J-H, Kuwano M. Polyoma middle T antigen or v-src desensitizes human epidermal growth factor receptor function and interference by a monensin-resistant mutation in mouse Balb/3T3 cells. Exp Cell Res, 1992;203:456–65.

23. Ettenberg SA, Magnifico A, Cuello M, et al. Cbl-b-dependent coordinated degradation of the epidermal growth factor receptor signaling complex. J Biol Chem, 2001;276:27677–84.

24. Barnes CJ, Bagheri-Yarmand R, Mandal M, et al. Suppression of epidermal growth factor receptor, mitogen-activated protein kinase, and Pak1 pathways and invasiveness of human cutaneous squamous cancer cells by the tyrosine kinase inhibitor ZD1839 (Iressa). Mol Cancer Ther, 2003;2:345–51.

Targeted disruption of one allele of the *Y-box binding protein-1* (*YB-1*) gene in mouse embryonic stem cells and increased sensitivity to cisplatin and mitomycin C

Kotaro Shibahara,[1,2] Takeshi Uchiumi,[1,7] Takao Fukuda,[1] Shinobu Kura,[3] Yohei Tominaga,[4] Yoshihiko Maehara,[2] Kimitoshi Kohno,[5] Yusaku Nakabeppu,[4] Teruhisa Tsuzuki[3] and Michihiko Kuwano[6]

[1]Departments of Medical Biochemistry, [2]Surgery and Science, [3]Medical Biophysics & Radiation Biology, [4]Faculty of Medical Sciences, Division of Neurofunctional Genomics, Medical, Institute of Bioregulation, Kyushu University, 3-1-1 Maidashi, Fukuoka 812-8582, [5]Department of Molecular Biology, University of Occupational and Environmental Health, Yahatanishi-ku, Kitakyushu 807-8555; and [6]Research Center for Innovative Cancer Therapy, 21st Century COE Program for Medical Science, Kurume University, 67 Asahimachi, Kurume, Fukuoka 830-0011

(Received January 7, 2004/Accepted February 4, 2004)

The eukaryotic Y-box binding protein-1 (YB-1) functions in various biological processes, including transcriptional and translational control, DNA repair, drug resistance, and cell proliferation. To elucidate the physiological role of the YB-1 protein, we disrupted one allele of mouse *YB-1* in embryonic stem (ES) cells. Northern blot analysis revealed that *YB-1*$^{+/-}$ ES cells with one intact allele contain approximately one-half the amount of mRNA detected in wild-type (*YB-1*$^{+/+}$) cells. We further found that the protein level of *YB-1*$^{+/-}$ cells was reduced to approximately 50–60% compared with that of *YB-1*$^{+/+}$ cells. However, no apparent growth difference was found between *YB-1*$^{+/-}$ and *YB-1*$^{+/+}$ cells. *YB-1*$^{+/-}$ cells showed increased sensitivity to cisplatin and mitomycin C, but not to etoposide, X-ray or UV irradiation, as compared to *YB-1*$^{+/+}$ cells. YB-1 may have the capacity to exert a protective role against cytotoxic effects of DNA damaging agents, and may be involved in certain aspects of drug resistance. (Cancer Sci 2004; 95: 348–353)

The Y-box protein family, which is widely distributed from bacteria to mammals, contains a cold-shock domain which is highly conserved from prokaryotic cold-shock proteins.[1] The human Y-box binding protein, YB-1, which is located on chromosome 1p34, was initially identified as a transcription factor which associates with the Y-box sequence appearing in the major histocompatibility complex class II genes.[2–4]

It has been hypothesized that YB-1 might play a role in promoting cell proliferation through the transcriptional regulation of various relevant genes, including proliferating cell nuclear antigen, epidermal growth factor receptor, DNA topoisomerase IIα, thymidine kinase, and DNA polymerase α.[5,6] In our laboratory, we have shown that YB-1 is involved in transcriptional activation of the human multidrug resistance 1 gene.[7–9] and also the DNA topoisomerase IIα gene[10] in response to various environmental stimuli. YB-1 appears to play a critical role in cell proliferation, DNA replication, and drug resistance. The biological roles of YB-1 include modification of chromatin, translational masking of mRNA, participation in the redox signaling pathway, RNA chaperoning, and stress response regulation.[11] It has also been demonstrated that eukaryotic Y-box proteins regulate gene expression at the translational level by recognizing RNA.[12,13] The murine YB-1 protein (MSY1) is specifically expressed in testis rather than other tissues, and regulates the translation of germ cell RNA.[14] The Y-box binding proteins thus appear to play critical roles in both mRNA turnover and translational control.

YB-1 also appears to protect mammalian cells from the cytotoxic effects induced by DNA damage. We have previously reported that human cancer cell lines overexpressing YB-1 showed resistance to cisplatin, while the reduction of YB-1 itself leads to increased drug sensitivity to cisplatin, other DNA-interacting drugs, and UV irradiation.[15] We also demonstrated that YB-1 protein is localized mainly in the cytoplasm, but translocates to the nucleus when cells are irradiated with UV or treated with anticancer drugs.[16] YB-1 specifically binds to cisplatin-modified DNA, apurinic DNA and also 8-oxo-guanine-containing RNA.[17–19] We have further demonstrated that YB-1 binds directly to repair-associated proteins such as proliferating cell nuclear antigen and p53 protein.[18,20] YB-1 may thus be involved in the process of DNA repair and/or DNA damage response. In clinical studies on YB-1, the cellular level of YB-1 was found to be closely associated with tumor growth and prognosis in ovarian cancers, lung cancers, and breast cancers.[21–23]

To gain more insight into how YB-1 proteins exert their multiple functions, we carried out a targeted disruption of the *mouse YB-1* gene (*MSY1*) in mouse embryonic stem (ES) cells. We have established ES cell lines with a heterozygously targeted disruption of the *YB-1* gene (*YB-1*$^{+/-}$), which we found to result in hypersensitivity to cytotoxic agents, such as cisplatin and mitomycin C.

Materials and Methods

Cell growth characteristics. CCE ES cells and YB-1 knockout cells were maintained on a feeder cell layer in DMEM supplemented with 20% heat-inactivated fetal bovine serum and 100 units/ml of recombinant leukemia inhibitory factor at 37°C in an atmosphere of 10% CO_2 in air.

Construction of the targeting vector. The mouse *YB-1* gene was isolated from a 129/Sv genomic library by the standard plaque hybridization method, using mouse *YB-1* cDNA as a probe. The targeting vector contained approximately 8.4 kb of genomic sequence interrupted by a *pol*II-*neo*-poly(A) cassette. Insertion of the neomycin (*neo*) cassette resulted in deletion of a 1.8-kb *SalI*/*Bgl*II fragment of the *YB-1* gene, containing 43 nucleotides of exon 5 and 84 nucleotides of exon 6, as well as 240 nucleotides of intron 5 and 1.4 kb of intron 6. A pair of herpes simplex virus thymidine kinase (TK) cassettes (TK1 and TK2, both under control of the MC1 promoter) were placed flanking

[7]To whom correspondence should be addressed.
E-mail: uchiumi@biochem1.med.kyushu-u.ac.jp
Abbreviations: YB-1, Y-box binding protein-1; ES, embryonic stem; MTS, [3-(4,5-dimethylthiazol-2-yl)-5-(3-carboxymethoxyphenyl)-2-(4-sulfophenyl)-2*H*-tetrazolium, inner salt; PES, phenazine ethosulfate.